ISBN: 978-81-993404-0-4

RAMACHANDRA
AUTONOMOUS

A BOOK OF
Engineering Epoxy-Based Glass Fiber Reinforced Hybrid Composites with Industrial Waste Fillers: Materials, Fabrication and Mechanical Performance

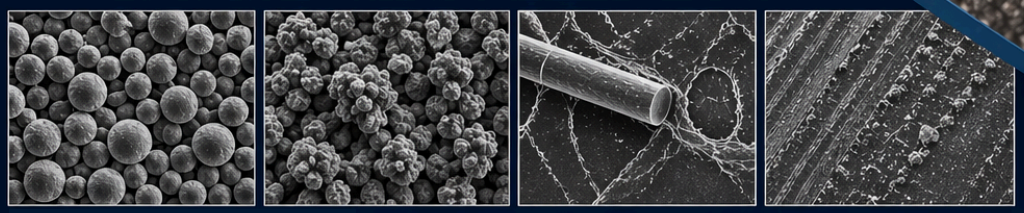

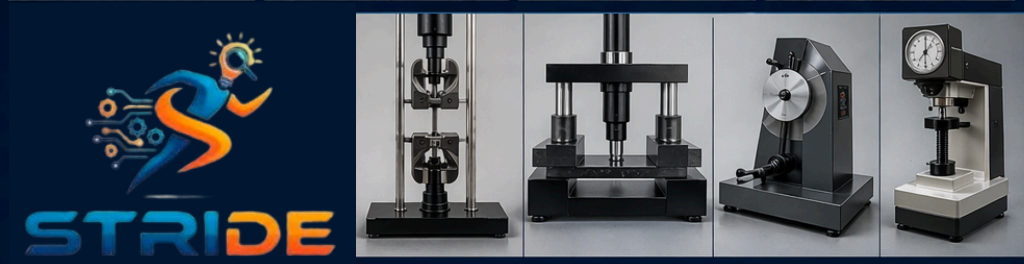

STRIDE

Authors
Dr. RAFFI MOHAMMED
Mr. ANGANI RAMACHANDU
Mr. SHAIK SOHEB KAREEM
Prof. B. SUDHAKARA RAO
Mr. MADHYANAPU SRINIVASA RAO
Mr. NARNI GANESH SIVA SHANKAR

Engineering Epoxy-Based Glass Fiber Reinforced Hybrid Composites with Industrial Waste Fillers: Materials, Fabrication and Mechanical Performance

Author(s)

Dr. Raffi Mohammed
Professor
Department of Mechanical Engineering
Ramachandra College of Engineering (A)
Eluru, Andhra Pradesh, India

Prof. B. Sudhakara Rao
Associate Professor&HoD
Department of Mechanical Engineering
Ramachandra College of Engineering (A)
Eluru, Andhra Pradesh, India

Mr. Angani Ramachandu
Department of Mechanical Engineering
Ramachandra College of Engineering (A)
Eluru, Andhra Pradesh, India

Mr. Shaik Soheb Kareem
Department of Mechanical Engineering
Ramachandra College of Engineering (A)
Eluru, Andhra Pradesh, India

Mr. Madhyanapu Srinivasa Rao
Department of Mechanical Engineering
Ramachandra College of Engineering (A)
Eluru, Andhra Pradesh, India

Mr. Narni Ganesh Siva Shankar
Department of Mechanical Engineering
Ramachandra College of Engineering (A)
Eluru, Andhra Pradesh, India

April-2026

Publisher:
The Institute for Innovations in Engineering and Technology
1-102, GP Street, Gurazada, Pamidimukkala
Mandal Krishna (Dt.), AP-521256,
Website: www.theiiet.com
E-Mail: contact@theiiet.com

ISBN 978-8-19-934040-4

THE INSTITUTE FOR INNOVATIONS IN ENGINEERING AND TECHNOLOGY

Published by **The Institute for Innovations in Engineering and Technology**
1-102, GP Street, Gurazada, Pamidimukkala Mandal, Krishna (Dt.), Andhra Pradesh-521256.

Title of the Book: ***Engineering Epoxy-Based Glass Fiber Reinforced Hybrid Composites with Industrial Waste Fillers: Materials, Fabrication and Mechanical Performance***, *April, Copyright © 2026 with Authors.*

Authors:

Dr. Raffi Mohammed, Professor, Department of Mechanical Engineering, Ramachandra College of Engineering(A), Eluru, Andhra Pradesh, India
Prof. B. Sudhakara Rao, Assoc. Professor&HoD, Department of Mechanical Engineering, Ramachandra College of Engineering(A), Eluru, Andhra Pradesh, India
Mr. Angani Ramachandu, Department of Mechanical Engineering, Ramachandra College of Engineering(A), Eluru, Andhra Pradesh, India
Mr. Shaik Soheb Kareem, Department of Mechanical Engineering, Ramachandra College of Engineering(A), Eluru, Andhra Pradesh, India
Mr. Madhyanapu Srinivasa Rao, Department of Mechanical Engineering, Ramachandra College of Engineering(A), Eluru, Andhra Pradesh, India
Mr. Narni Ganesh Siva Shankar, Department of Mechanical Engineering, Ramachandra College of Engineering(A), Eluru, Andhra Pradesh, India

ISBN 978-8-19-934040-4

Typeset at the IIET, D: 1-102, GP Street, Vijayawada-521256.
Printed and bounded in India at Printster.in, S-548A, 1st Floor, School Block, Shakarpur, Laxmi Nagar, Delhi, 110092, India
Visit us at: www.theiiet.com ; Phone: 91-9533111789;
Write to us at: contact@theiiet.com

Acknowledgements

The authors take immense pleasure in expressing their sincere gratitude to all individuals and institutions whose unwavering support, guidance, and encouragement have contributed to the successful completion of this work on *"Engineering Epoxy-Based Glass Fiber Reinforced Hybrid Composites with Industrial Waste Fillers: Materials, Fabrication and Mechanical Performance"* This work represents a collaborative academic effort grounded in systematic experimentation, scientific inquiry, and a shared vision toward advancing sustainable and high-performance composite materials for engineering applications.

The authors express their profound appreciation to the Management of **Ramachandra College of Engineering (Autonomous), Eluru, Andhra Pradesh, India**, for their visionary leadership, continuous encouragement, and commitment to fostering a strong culture of research, innovation, and academic excellence. The institutional support, infrastructure, and conducive research environment provided have played a vital role in enabling the successful execution of this work.

The authors extend their deepest gratitude to **Dr. M. Muralidhara Rao**, Director & Principal, for his exceptional leadership, constant encouragement, and valuable insights that have significantly enriched the quality of this research. His commitment to promoting interdisciplinary research and innovation has been a continuous source of inspiration.

The authors also wish to acknowledge the academic guidance and encouragement extended by the Deans and academic leadership of the institution, whose support has greatly contributed to strengthening the research orientation and scholarly depth of this work.

Special appreciation is extended to the faculty members and technical staff of the Department of Mechanical Engineering for their constant support, valuable suggestions, and technical assistance throughout the various stages of this work. Their cooperation in facilitating laboratory work, material procurement, and experimental setup has been instrumental in ensuring the smooth progress of this research.

The authors gratefully acknowledge the contributions of the broader research community in the field of composite materials and sustainable engineering. The extensive body of knowledge developed by researchers in polymer matrix composites, hybrid reinforcement systems, and industrial waste utilization has provided a strong foundation and direction for the present work. Their pioneering efforts continue to inspire advancements in environmentally responsible material development.

The authors further recognize the importance of industrial by-product utilization, particularly coal fly ash and silica fume, in promoting sustainable engineering practices. This work is a modest contribution toward the effective utilization of such materials in developing high-performance composites while addressing environmental concerns associated with waste disposal.

Finally, the authors express their heartfelt gratitude to their families, friends, and well-wishers for their continuous moral support, encouragement, and motivation throughout the course of this work. Their belief and encouragement have been a constant source of strength and inspiration.

-Authors

Preface

Composite materials have emerged as one of the most significant classes of engineering materials in modern science and technology, offering exceptional strength-to-weight ratios, durability, and design flexibility. Among these, polymer matrix composites—particularly epoxy-based systems reinforced with glass fibers—have gained widespread acceptance in structural, automotive, aerospace, and industrial applications. In recent years, the integration of industrial by-products into composite systems has attracted considerable attention due to the dual advantages of performance enhancement and environmental sustainability.

This work, titled *"Engineering Epoxy-Based Glass Fiber Reinforced Hybrid Composites with Industrial Waste Fillers: Materials, Fabrication and Mechanical Performance"* is an outcome of systematic research focused on the development, fabrication, and mechanical performance evaluation of hybrid composites incorporating coal fly ash and silica fume as particulate fillers. These materials, traditionally considered industrial waste, possess significant potential to improve mechanical properties while contributing to sustainable material development through effective waste utilization.

The primary objective of this work is to investigate the influence of varying weight fractions of fly ash and silica fume on the mechanical behaviour of epoxy-based glass fiber reinforced composites. The study encompasses fabrication using the hand lay-up technique, followed by detailed mechanical characterization including tensile strength, flexural strength, impact resistance, and hardness in accordance with ASTM standards. Furthermore, the work adopts a systematic approach to identify optimal compositions and understand the underlying material behaviour through experimental analysis.

A key motivation behind this work is to bridge the gap between conventional composite development and sustainable engineering practices. By incorporating industrial by-products into high-performance composite systems, this study contributes to the growing body of research aimed at reducing environmental impact while maintaining or enhancing material performance. The findings presented herein are expected to provide valuable insights for researchers, academicians, and practicing engineers engaged in the field of composite materials and advanced manufacturing.

This work is organized in a structured manner, beginning with fundamental concepts and literature review, followed by detailed methodology, experimental investigation, results analysis, and concluding with key findings and future research directions. Every effort has been made to present the content in a clear, systematic, and academically rigorous manner.

The authors sincerely hope that this work will serve as a useful reference for students, researchers, and professionals interested in hybrid composites, sustainable materials, and advanced manufacturing techniques. It is also envisioned that this contribution will encourage further research in the area of industrial waste utilization in high-performance engineering materials.

Foreword

The field of composite materials has undergone remarkable transformation over the past few decades, evolving from conventional fiber-reinforced systems to highly engineered, multifunctional materials tailored for demanding applications. Among these, epoxy-based glass fiber reinforced composites have established themselves as indispensable materials across structural, automotive, aerospace, and industrial sectors due to their superior mechanical performance, corrosion resistance, and adaptability in design. However, the growing emphasis on sustainability and resource efficiency has necessitated a paradigm shift toward the incorporation of eco-friendly and waste-derived materials into advanced composite systems.

The book titled “Engineering Epoxy-Based Glass Fiber Reinforced Hybrid Composites with Industrial Waste Fillers: Materials, Fabrication and Mechanical Performance” represents a timely and significant contribution to this evolving domain. It successfully bridges the gap between traditional composite engineering and modern sustainability-driven approaches by exploring the integration of industrial by-products such as coal fly ash and silica fume into high-performance polymer composites.

This work stands out for its systematic and comprehensive treatment of the subject, beginning with fundamental material concepts and progressing through fabrication techniques, experimental methodologies, and detailed mechanical characterization. The authors have demonstrated a strong command over both theoretical and practical aspects of composite materials, presenting their findings with clarity, technical depth, and scientific rigor. The inclusion of standardized testing methods and analytical approaches further enhances the reliability and applicability of the results.

One of the notable strengths of this book lies in its focus on hybrid composite systems, where the synergistic interaction between fiber reinforcement and particulate fillers is effectively utilized to enhance performance. The utilization of industrial waste materials not only contributes to improved mechanical properties but also addresses critical environmental concerns associated with waste disposal and resource depletion. This aligns well with global efforts toward sustainable engineering and circular economy practices.

The insights presented in this book are expected to be of great value to researchers, academicians, practicing engineers, and industry professionals working in the fields of composite materials, advanced manufacturing, and sustainable engineering. It also serves as an excellent reference for postgraduate students and scholars seeking to explore emerging trends in hybrid composite development and performance optimization.

In conclusion, this book reflects a commendable effort by the authors in advancing both the scientific understanding and practical application of epoxy-based hybrid composites. It is hoped that this work will inspire further research, innovation, and industrial adoption of sustainable composite materials for future engineering applications.

Dr. Abdul Saddique Shaik
Faculty of Mechanical Engineering
King Khalid University
Abha, Saudi Arabia

Table of Contents

LIST OF FIGURES

LIST OF TABLES

ABSTRACT

E-glass fibre reinforced epoxy composites occupy a dominant position in structural applications due to their excellent strength-to-weight ratio, corrosion resistance, and cost-effectiveness. The incorporation of industrial by-product fillers such as fly ash (FA), obtained from coal-fired power plants, and silica fume (SF), generated from silicon alloy furnaces, offers a dual advantage of enhancing mechanical performance through microstructural modification while simultaneously addressing environmental concerns associated with solid waste disposal. However, the combined or synergistic effect of incorporating both FA and SF as particulate fillers in fibre-reinforced polymer composites has not been comprehensively investigated across a full range of mechanical properties.

In the present study, E-glass fibre reinforced epoxy hybrid composites were fabricated using LY556 epoxy resin through the manual hand lay-up technique. A systematic experimental design was adopted by incorporating Class F fly ash and undensified silica fume at varying weight fractions of 2.5%, 5%, 7.5%, and 10%, resulting in multiple composite formulations. The fabricated laminates were cured at room temperature for 24 hours followed by post-curing at 60°C for 4 hours to ensure proper cross-linking of the matrix. Standard test specimens were prepared from the laminates and evaluated for tensile strength (ASTM D638), flexural strength (ASTM D790), impact strength (ASTM D256), and Vickers micro hardness (ASTM E384).

The experimental results revealed that the incorporation of fillers significantly improves the mechanical properties up to an optimal filler content of 5 wt%, beyond which performance declines due to particle agglomeration and reduced interfacial bonding. Among all compositions, the composite containing 5 wt% silica fumes exhibited the best mechanical performance, achieving a tensile strength of 345 MPa, flexural strength of 470 MPa, inter-laminar shear strength of 28.5 MPa, and impact strength of 77 kJ/m². Vickers micro hardness increased progressively with filler content, reaching a maximum value of 122 HV at higher loadings.

To identify the most suitable composite considering multiple mechanical criteria simultaneously, the Technique for Order Preference by Similarity to Ideal Solution (TOPSIS) was employed. The analysis indicated that the optimal composite achieved the highest closeness coefficient (Ci = 0.92), confirming its superior overall performance. The study

further highlights the effectiveness of silica fume over fly ash in improving interfacial bonding and load transfer characteristics due to its finer particle size and higher surface area.

The findings of this research demonstrate that the integration of industrial waste fillers with fibre-reinforced composites not only enhances mechanical performance but also contributes to sustainable material development. The optimized composite is strongly recommended for structural applications, particularly in rail joint fabrication, where high strength, durability, and resistance to dynamic loading are critical.

Keywords:

E-glass fibre; epoxy matrix; fly ash; silica fume; hybrid composite; hand lay-up; tensile strength; flexural strength; impact strength; Hardness, TOPSIS

CHAPTER 1
INTRODUCTION

1.1 Background of Composite Materials

A composite material is a multiphase material system in which two or more distinct constituent phases are combined at the macroscopic level to form a new material whose properties surpass those of either constituent acting alone. The idea of combining materials to exploit complementary attributes is as old as civilisation itself: ancient Mesopotamian builders reinforced mud bricks with straw to prevent cracking, Egyptian craftsmen laminated wood in alternating grain directions to produce dimensionally stable panels, and Mongol warriors fabricated recurve bows from layers of horn, wood, and sinew bonded with natural glue [1]. Despite this long empirical heritage, the scientific discipline of composite materials engineering emerged formally only in the twentieth century, driven by the demands of the aerospace and defence industries for structural materials that are simultaneously lightweight, stiff, strong, and durable.

The modern era of engineered composites began in the 1940s with the development of glass-reinforced unsaturated polyester (GRP), which offered unprecedented specific stiffness compared to sheet metal. The subsequent introduction of carbon fibre in the 1960s, aramid (Kevlar) fibre in the 1970s, and sophisticated thermoset epoxy resin systems in the 1980s steadily elevated the performance envelope of FRP composites, enabling their adoption in primary aircraft structures, wind turbine blades, high-performance automotive components, and civil engineering infrastructure [2,3].

The global fibre-reinforced polymer composites market was valued at approximately USD 110 billion in 2022 and is projected to reach USD 194 billion by 2030, growing at a compound annual growth rate (CAGR) of 7.3% [4]. This growth is driven primarily by increasing light weighting requirements in automotive and aerospace sectors—spurred by stringent CO2 emissions regulations-and by the explosive growth of wind energy, where each modern offshore turbine blade requires 15–25 tonnes of composite material. The construction sector is also a rapidly expanding end-user, employing FRP in bridge decks, rebars, blast-resistant panels, and retrofitting of heritage structures.

Composite materials are most broadly classified according to the geometry of the reinforcing phase: (i) fibrous composites, in which the reinforcement is in the form of

continuous or chopped fibres; (ii) particulate composites, in which the reinforcement is spherical, irregular, or platelet-shaped particles; and (iii) laminated composites, in which sheets of different materials are bonded together. Hybrid composites combine elements of two or more of these categories. A second classification is by matrix type: polymer matrix composites (PMCs), metal matrix composites (MMCs), and ceramic matrix composites (CMCs). Table 1.1 summarises this classification with representative material systems and application domains.

Table 1.1: Classification of Engineering Composite Materials by Matrix and Reinforcement Type [1-4]

Matrix Category	Matrix Material	Typical Reinforcement	Key Applications
PMC	Epoxy, Polyester, Vinylester, PEEK	Glass, Carbon, Aramid, Natural fibres	Aerospace, Automotive, Marine, Sport
MMC	Al, Ti, Mg, Cu alloys	SiC, Al_2O_3, Boron, C fibres	Engine parts, Brake discs, Armour
CMC	Al_2O_3, SiC, Si_3N_4	SiC fibres, Carbon fibres	Jet engines, Re-entry vehicles, Cutting tools
Hybrid	Epoxy (most common)	Glass + Carbon, FA + SF + Glass	Structural panels, Industrial equipment

The mechanics governing composite behaviour can be understood at three scales: (i) the micro-mechanical scale, which analyses stress distribution within and around individual fibres and particles; (ii) the meso-mechanical scale, which considers the behaviour of a single lamina or ply; and (iii) the macro-mechanical scale, which treats the laminate as a homogeneous anisotropic medium and predicts structural response under applied loads. Classical Lamination Theory (CLT) links these scales and provides the analytical framework for designing composite laminates with tailored stiffness and strength [5]. The present work primarily addresses the micro- and meso-mechanical scales through experimental characterisation of composite formulations with systematically varied filler compositions.

Environmental sustainability has emerged as a critical consideration in composite material design. The use of industrial by-products—such as fly ash and silica fume—as matrix fillers aligns with the principles of the circular economy, transforming waste streams into value-added material inputs. India generates over 220 million tonnes of fly ash annually from coal-fired thermal power plants, of which approximately 33% remains unutilised and is deposited in ash ponds, occupying vast tracts of land and posing groundwater contamination

risks [6]. Incorporating fly ash and silica fume into high-performance composite laminates represents a technically sound and environmentally responsible strategy for waste valorisation.

1.2 Polymer Matrix Composites (PMCs)

Polymer Matrix Composites constitute the largest and most commercially significant sub-class of composite materials. The polymer matrix fulfils four essential functions in a PMC: (i) binding the reinforcing fibres into a coherent structural form; (ii) transferring applied loads to the reinforcing fibres through interfacial shear stress; (iii) protecting the fibres from mechanical damage during handling and service; and (iv) governing the transverse and inter-laminar shear properties of the composite, which are often the design-limiting failure modes in laminates. The choice of matrix therefore exerts a profound influence on processability, service temperature capability, toughness, and durability.

Thermoset polymers-which cure irreversibly by cross-linking reactions to form a three-dimensional molecular network—are the dominant matrix materials for structural PMCs. Epoxy resins are the preferred thermoset for high-performance structural applications. The workhorse epoxy system is based on the diglycidyl ether of bisphenol A (DGEBA), which is cured with aliphatic amine hardeners such as triethylenetetramine (TETA) or aromatic amines such as 4,4'-diaminodiphenylsulphone (DDS). The specific resin system used in this investigation, LY556/ HY951 (Huntsman Corporation), is one of the most widely characterised epoxy formulations in the open literature, offering a tensile modulus of approximately 3.7 GPa, tensile strength of 75–80 MPa, glass transition temperature (Tg) of approximately 120°C, and excellent adhesion to glass fibres in the uncured state [7].

Key advantages of epoxy matrices relative to competing thermosets (polyester, Vinylester) include: negligible cure shrinkage (<3% vs. 6–8% for polyester), superior fibre-matrix adhesion, higher Tg, and better resistance to moisture and chemical attack. Key disadvantages include higher cost, longer cure cycle, brittleness (fracture toughness KIc ~0.5–0.8 MPa√m for neat resin), and the need for careful stoichiometric control of the hardener ratio [8].

Thermoplastic polymer matrices—such as PEEK, PPS, and nylon—offer inherent toughness and recyclability advantages but require significantly higher processing temperatures and pressures, limiting their use in large-structure fabrication by conventional methods. The present study employs a thermoset epoxy matrix for its superior fibre-matrix adhesion, ease of

hand lay-up processing at ambient temperature, and established property database in the open literature.

1.3 E-Glass Fiber Reinforcement

E-Glass (Electrical-grade glass) fibre is the most commercially important reinforcing fibre in the global composites industry, accounting for approximately 90% of all glass fibre consumed by volume [9]. It is produced by drawing molten borosilicate glass—melted from silica sand (SiO_2), limestone ($CaCO_3$), alumina (Al_2O_3), boric oxide (B_2O_3), and fluxing agents—through platinum-rhodium bushing tips at temperatures of 1250–1380°C into continuous filaments of 5–24 µm diameter. The freshly drawn filaments are immediately quenched by a water spray, coated with an organosilane-based chemical sizing agent, and wound onto forming packages.

The chemical sizing agent serves two critical functions: it promotes wetting and adhesion between the glass surface and the polymer matrix (typically through a silane coupling agent, such as gamma-aminopropyltriethoxysilane, which bonds covalently to both the silanol groups on the glass surface and the amine groups in the epoxy matrix), and it lubricates the filaments to prevent inter-filament abrasion during subsequent textile processing into woven fabrics, rovings, or mats [10].

Plain-weave E-glass woven fabric—used in this study—is the most common architectural form for hand lay-up laminates. In a plain weave, each warp yarn passes alternately over and under each weft yarn, providing equal properties in the 0° and 90° directions. The high degree of fibre crimp in plain weave (relative to satin or twill weave) reduces the in-plane tensile modulus somewhat but imparts excellent inter-laminar toughness due to the mechanical interlocking of yarns. The fabric used in this study has an areal weight of 300 g/m² and a balanced plain weave construction. A comparative summary of the physical and mechanical properties of E-glass fibres with other commercial reinforcements is presented in Table 1.2.

Table 1.2: Physical and Mechanical Properties of E-Glass Fibres Compared with Other Commercial Reinforcements [9-10]

Property	E-Glass	S-Glass	Carbon (HM)	Aramid (Kevlar 49)	Unit
Tensile Strength	3,400	4,580	3,800	3,600	MPa
Tensile Modulus	72.4	86.9	380	125	GPa
Density	2.54	2.49	1.80	1.44	g/cm³
Elongation at Break	4.8	5.7	0.6	2.8	%
CTE (axial)	5.0	2.9	-0.5	-2.0	µm/m·°C
Relative Cost	Low	Moderate	Very High	High	—
Key Advantage	Low cost, good all-round properties	High strength	Ultra-high stiffness	High tensile strength, low density	—

1.4 Role of Fillers in Composites

Particulate fillers are solid, discrete secondary phases incorporated into a composite matrix to modify its properties without fundamentally changing the primary load-bearing architecture. Their influence on composite performance is multifaceted and encompasses mechanical, thermal, electrical, optical, and economic dimensions. In the context of FRP structural composites, the mechanical roles of fillers are of primary interest and can be categorised as follows:

1. Crack arrest and toughening: Rigid micro-particles intercept advancing cracks and force them to deflect around the particle, dissipating fracture energy. This mechanism, known as crack deflection, has been quantitatively modelled by Evans [11] and Lange [12] and has been demonstrated experimentally for silica, alumina, and glass hollow sphere fillers in epoxy matrices.
2. Matrix stiffening: Filler particles with modulus higher than the matrix contribute to increased composite stiffness. For spherical particles in a continuous matrix, the Kerner model and Halpin–Tsai equations provide widely used predictions of modulus enhancement as a function of particle volume fraction and modulus ratio.
3. Void filling and densification: Ultra-fine fillers (<10 µm) occupy the inter-fibre spaces in FRP composites that would otherwise form voids during wet hand lay-up. Void

content reduction is a primary mechanism by which SF improves composite properties in the present study, as voids act as stress concentrators and as initiation sites for delamination.

4. Wear and hardness improvement: Harder filler particles (FA hardness ~5–6 Mohs) distribute contact stress and resist ploughing by abrasive counterfaces, improving tribological performance.
5. Thermal management: Mineral fillers such as alumina and silica increase thermal conductivity (advantageous for heat dissipation) and can increase the heat distortion temperature (HDT) of the composite.
6. Water barrier effect: Dense, glassy filler particles increase the tortuosity of moisture diffusion pathways through the composite cross-section, reducing the equilibrium water uptake and the rate of moisture ingress—a critical durability parameter for composites in humid or marine environments.

The effectiveness of a filler is critically dependent on the quality of its dispersion within the matrix. Poor dispersion—manifested as agglomeration of particles into clusters—creates large stress-concentrating in homogeneities that can negate the intended reinforcing effect. Achieving adequate dispersion of ultra-fine fillers such as SF (mean diameter ~0.15 µm) in a viscous epoxy resin requires prolonged mechanical stirring or high-shear mixing, followed by ultrasonic treatment and de-airing. The fabrication protocol adopted in this study incorporates all three steps to maximise dispersion quality.

1.5 Fly Ash as a Filler

Fly ash (FA) is a fine particulate by-product collected from the electrostatic precipitators or fabric filter systems of coal-fired thermal power plants. When pulverised coal is burned in a furnace at ~1400°C, the mineral impurities in the coal fuse into droplets that are rapidly quenched in the exhaust gas stream, solidifying into glassy, predominantly spherical particles that are carried upward with the flue gas. The particle size distribution of fly ash is broad, typically ranging from 1 to 150 µm, with a median particle diameter (d50) of approximately 15–25 µm depending on the coal source and combustion conditions [6].

The mineralogical composition of fly ash varies with the rank of the parent coal. Class F fly ash, produced from bituminous and anthracite coals, is predominantly amorphous (60–80% amorphous SiO_2-Al_2O_3 glass), with minor crystalline phases including quartz (SiO_2),

mullite (3Al2O3·2SiO2), magnetite (Fe3O4), and hematite (Fe2O3). Class C fly ash, from sub-bituminous and lignite coals, contains significantly higher CaO content (>20%) and exhibits both pozzolanic and hydraulic (self-cementing) reactivity. Figure 1.1 shows a schematic XRD pattern characteristic of Class F fly ash, illustrating the broad amorphous hump centred around 2θ = 22° and the crystalline diffraction peaks of quartz and mullite.

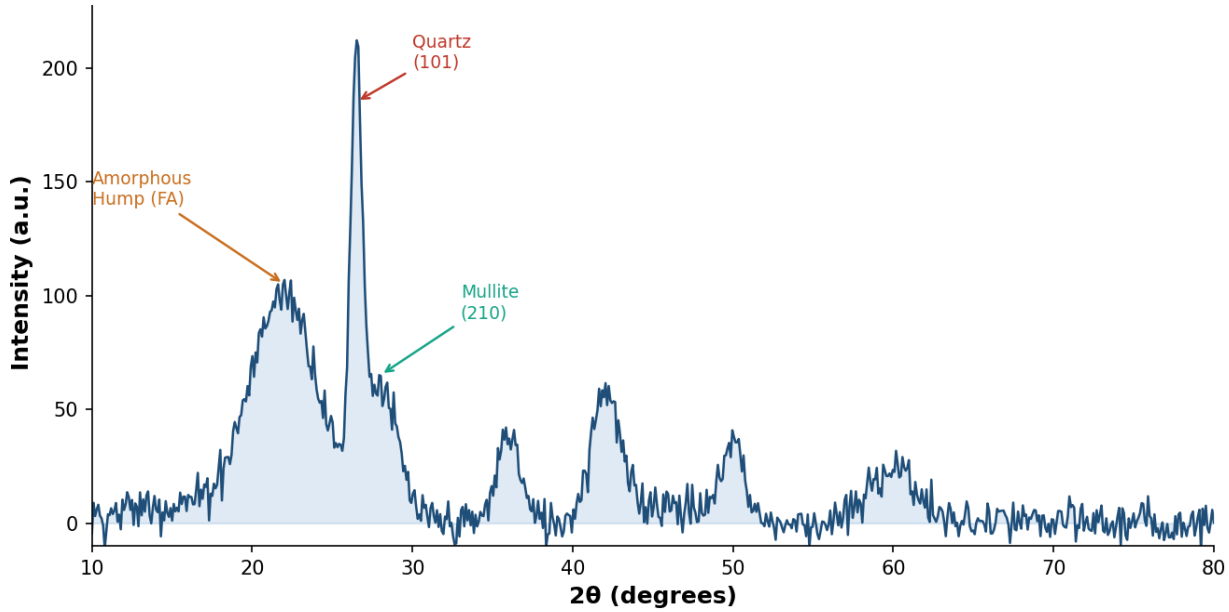

Figure 1.1: Schematic XRD Pattern of Class F Fly Ash Showing Amorphous Hump and Crystalline Phases

A notable morphological feature of fly ash is the presence of cenospheres—hollow, thin-walled glassy spheres of density 0.4–0.8 g/cm³, formed when gas is trapped inside the molten droplet during rapid solidification. Cenospheres constitute 0.5–3% of fly ash by weight but are highly valued for producing lightweight syntactic foams and low-density composite fillers. The solid glass spheres (density 2.0–2.4 g/cm³) constitute the bulk of fly ash and are the particles primarily responsible for the mechanical property modifications reported in this study.

From a processing standpoint, fly ash reduces the viscosity of epoxy resin/filler suspensions (relative to angular or platelet fillers of comparable volume fraction) due to the smooth spherical morphology of its particles—a phenomenon known as the 'ball-bearing effect' that facilitates resin impregnation during hand lay-up. The chemical inertness of fly ash glass with respect to epoxy resins means that no covalent bonding occurs at the fly ash–epoxy interface without surface treatment; interfacial adhesion in untreated systems relies on van der Waals forces and mechanical interlocking. Surface silylation with silane coupling agents (e.g., APTES or GPTMS) has been shown to significantly improve interfacial bonding and composite mechanical properties [13].

1.6 Silica Fume as a Filler

Silica fume (SF), also designated micro silica or condensed silica fume, is an ultra-fine amorphous silicon dioxide (SiO2) by-product generated in electric arc furnaces during the production of ferrosilicon and silicon metal. Reduction of high-purity quartz (SiO2) with coal or coke at temperatures exceeding 2000°C produces SiO gas that rises from the furnace, is oxidised to SiO2 in the upper, cooler regions of the furnace, and condenses to form fine spherical amorphous particles that are collected by bag filters [14]. Undensified silica fume has a bulk density of only 130–430 kg/m³ and a BET specific surface area of 15,000–25,000 m²/kg, reflecting the ultra-fine particle size of 0.05–1 µm (mean ~0.15 µm).

The high amorphous SiO2 content (typically 85–98%) and enormous surface area give silica fume its exceptional pozzolanic reactivity. In cement-based materials, SF reacts with Ca(OH)2 liberated by cement hydration to form additional calcium silicate hydrate (C-S-H), filling capillary pores and significantly improving strength, durability, and impermeability-a property known as the 'micro-filler effect'. In polymer composites, analogous mechanisms operate through chemical and physical interaction with the matrix: the abundant surface silanol groups (Si-OH) of amorphous silica can react with amine groups of the epoxy hardener or with silane coupling agents applied to the SF surface, creating covalent cross-links between the filler and the matrix that dramatically improve interfacial load transfer [15].

A practical challenge in using SF in polymer composites is its extreme tendency to agglomerate due to van der Waals forces and electrostatic attractions between the ultra-fine particles. Agglomerates of SF behave as large, weak, porous clusters rather than as dense, hard reinforcing particles, and their presence dramatically reduces the improvement in mechanical properties. The de-agglomeration protocol used in this study—sequential mechanical stirring (30 min), three-roll mill processing, and ultrasonic bath treatment (30 min, 40 kHz)—is designed to ensure maximum dispersion quality before combining the SF-loaded resin with fly ash and the hardener. A comparative summary of the physico-chemical properties of fly ash and silica fume used in this study is presented in Table 1.3.

Table 1.3: Physico-Chemical Properties of Fly Ash and Silica Fume Used in This Study

Property	Class F Fly Ash	Silica Fume (Grade 920U)
SiO_2 Content (%)	52.4	93.8
Al_2O_3 (%)	28.1	0.4

Fe_2O_3 (%)	9.2	0.9
CaO (%)	3.6	0.3
Mean Particle Size (µm)	18.4	0.15
Specific Gravity	2.14	2.22
Specific Surface Area (m^2/kg)	380	18,500
Colour	Light grey to tan	Off-white to light grey
Crystallinity	Semi-crystalline (Quartz, Mullite)	Amorphous (>95%)

1.7 Hybrid Composites

The term 'hybrid composite' denotes a material system incorporating two or more distinct types of reinforcing constituents within a single matrix. Hybridisation exploits the complementary attributes of different reinforcements to produce performance profiles that are unachievable with a single reinforcement type. The concept was first formalised by Bunsell and Harris [16] in 1974 through the discovery of the 'hybrid effect'—the observation that the failure strain of the lower-elongation constituent (typically carbon fibre, in carbon-glass hybrids) is enhanced in the hybrid laminate beyond what would be predicted by the rule of mixtures. This strain enhancement arises because the high-elongation constituent (glass fibre) constrains the spread of damage in the low-elongation constituent, delaying catastrophic failure.

In the present study, hybridisation operates on two distinct length scales. At the macro-scale, the woven E-glass fabric provides the primary structural reinforcement, carrying tensile and flexural loads through continuous fibre bundles that span the full laminate width. At the micro-scale, the dual particulate fillers-fly ash (d50 ~18 µm) and silica fume (d50 ~0.15 µm)—modify the epoxy matrix micro-structure, filling inter-fibre voids, strengthening the fibre-matrix interphase, and deflecting advancing matrix cracks. This length-scale separation means that the micro-scale fillers do not directly compete with the macro-scale fibres for load-bearing duty; rather, they enhance the matrix-dominated properties (transverse strength, inter-laminar shear strength, impact toughness, and water resistance) while the fibres govern the longitudinal tensile and flexural properties [17].

The optimal filler content in hybrid composites is governed by a balance between reinforcing benefits and agglomeration-related penalties. At low filler loading, the number of crack-deflecting particles and void-filling particles is insufficient to produce significant

property improvements. At high filler loading, inter-particle interactions lead to agglomerate formation, the increase in resin viscosity degrades fibre impregnation quality, and the total volume of load-bearing epoxy matrix is reduced. The crossover between net benefit and net detriment has been reported in the range of 15–25 wt% for micrometre-scale FA and 8–12 wt% for sub micrometre-scale SF in epoxy composites. This range frames the experimental design of the present investigation [18].

1.8 Problem Statement

Despite extensive research on individual filler additions to E-glass/epoxy composites, the following specific problem remains insufficiently addressed in the published literature: the effect of simultaneously adding both Class F fly ash and undensified silica fume as dual particulate fillers—at systematically varied weight fractions—on the full mechanical property profile (tensile, flexural, impact, hardness, and water absorption) of woven E-glass/epoxy laminates fabricated by the hand lay-up process.

From an industrial standpoint, the ability to predict and optimise composite formulations combining locally sourced industrial wastes (FA from nearby thermal power stations; SF from ferro-silicon producers) with commercially available E-glass fabric and standard epoxy resins would provide SME composite fabricators with a technically validated, economically attractive, and environmentally sustainable product formulation. The present study directly addresses this need.

1.9 Objectives of the Study

The key objectives of the present study are summarized in Figure 1.2 and detailed as follows:

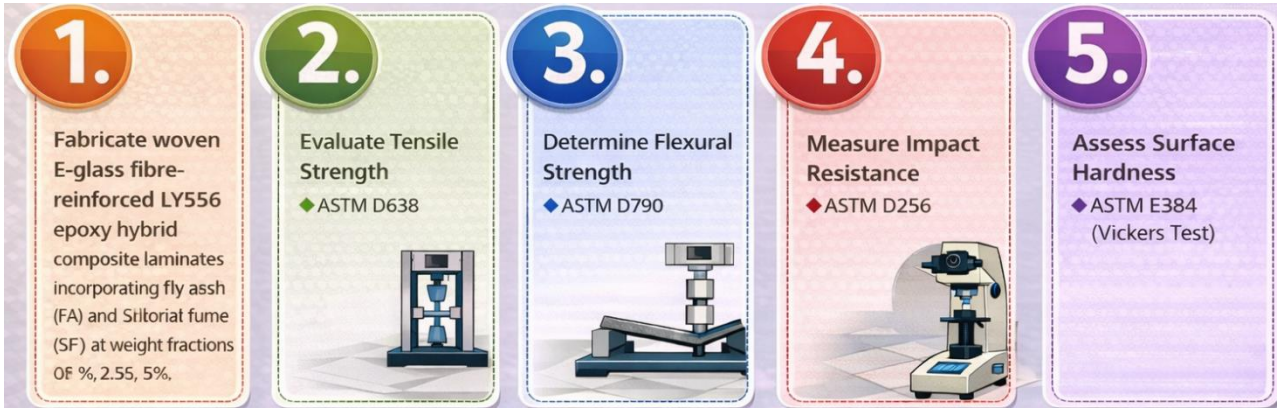

Figure 1.2: Objectives of the Study

1. To fabricate woven E-glass fiber reinforced LY556 epoxy hybrid composite laminates incorporating fly ash (FA) and silica fume (SF) at weight fractions of 0%, 2.5%, 5%, 7.5%, and 10% using the hand lay-up technique, based on a full factorial experimental design.
2. To evaluate the tensile strength of all composite formulations in accordance with ASTM D638-III standards.
3. To determine the flexural strength using the three-point bending test as per ASTM D790.
4. To measure the impact resistance of the composites through Izod notched impact testing in accordance with ASTM D256.
5. To assess the surface hardness of the developed composites using the Vickers Micro hardness test as per ASTM E 384.

1.10 Scope of the Study

The scope of the present investigation is centered on the development and evaluation of sustainable composite materials through the incorporation of industrial waste fillers, namely fly ash (FA) and silica fume (SF), into woven E-glass fiber reinforced LY556 epoxy laminates. This study emphasizes the effective utilization of these waste by-products to reduce environmental burden, minimize landfill disposal, and promote resource efficiency in material engineering. The fabrication of composite laminates is carried out using the hand lay-up technique, ensuring a cost-effective and scalable approach suitable for sustainable manufacturing practices.

From a research perspective, the study systematically investigates the influence of varying filler weight fractions on the mechanical performance of the composites, including tensile strength, flexural strength, impact resistance, and surface hardness, as per relevant ASTM standards. The work aims to establish a balance between mechanical performance and environmental benefits by identifying optimal filler compositions that enhance material properties while contributing to waste valorization.

Additionally, the study explores the potential of these eco-friendly composites as viable alternatives to conventional materials in engineering applications, thereby supporting the transition toward greener and more sustainable material systems. While the current investigation focuses on mechanical characterization under controlled laboratory conditions, it

lays the foundation for future research on life cycle assessment, long-term environmental impact, and large-scale industrial implementation of sustainable composite materials.

1.11 Organization of the Thesis

This project report is organised into five chapters, as follows:

1. Chapter 1 (Introduction): Provides the conceptual and contextual background for the study, covering composite material classification, PMC and E-glass fibre fundamentals, the role of particulate fillers, the characteristics of fly ash and silica fume, the hybrid composite concept, and the problem statement, objectives, scope, and thesis organisation.
2. Chapter 2 (Literature Review): Critically surveys published research on E-glass/epoxy composites, fly ash-filled composites, silica fume-filled composites, and hybrid multi-filler systems. Fabrication methods and applicable ASTM test standards are reviewed. The chapter concludes with an identification of the specific research gaps addressed by this investigation.
3. Chapter 3 (Materials and Methodology): Describes in detail the materials used, the hand lay-up fabrication protocol, laminate curing and post-curing, specimen geometry preparation, and mechanical testing procedures
4. Chapter 4 (Results and Discussion): Presents and critically analyses all experimental results for tensile properties, flexural properties, impact strength, Vickers micro hardness and inter-laminar shear strength. Mechanisms underlying the observed trends are discussed with reference to relevant literature.
5. Chapter 5 (Conclusions and Future Work): Summarises the principal findings, states the contributions to engineering knowledge, acknowledges the limitations of the study, and recommends specific directions for future research to build upon this work.

The report is followed by a complete list of 55+ references in journal-standard format.

CHAPTER-2
LITERATURE REVIEW

2.1 Overview of Previous Research

The scientific literature on fibre-reinforced polymer composites is vast, with over 50,000 archival journal articles published as of 2024 in indexed databases such as Scopus, Web of Science, and Google Scholar. Figure 2.1, illustrates the growth in research publications specifically addressing glass fibre hybrid composites with particulate fillers between 2005 and 2024, showing a clear exponential trend with an approximate doubling of annual output every five years. This growth is paralleled by advances in characterisation tools (high-resolution SEM/TEM, nano-indentation, micro-CT tomography) and modelling approaches (molecular dynamics, multi-scale finite element analysis) that have provided increasingly detailed mechanistic insight into composite behaviour.

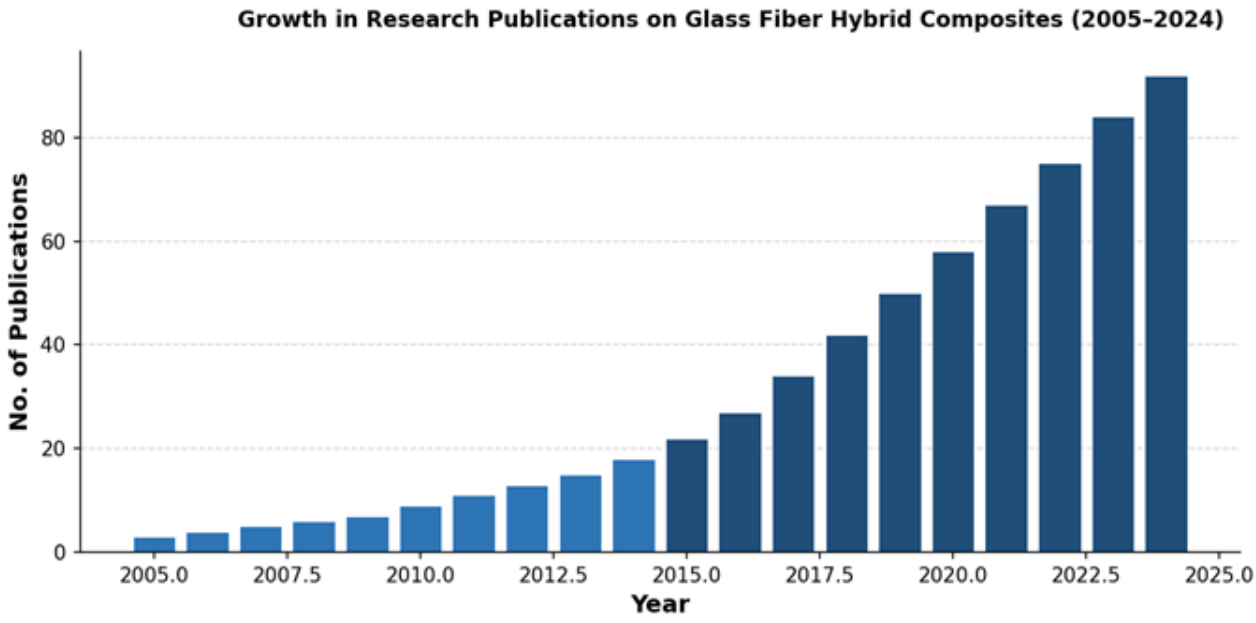

Figure 2.1: Growth in Research Publications on Glass Fibre Hybrid Composites with Mineral Fillers (2005–2024). Source: Scopus database analysis, keyword: 'glass fiber + epoxy + filler + hybrid composite'.

Early foundational texts by Ashby and Jones [1], Mallick [3], and Daniel and Ishai [5] established the theoretical and experimental framework for composite materials science that underpins current research. The review by Friedrich and Almajid [19] synthesised the role of micro- and nano-fillers in improving tribological performance of polymer composites, while

Cho et al. [20] provided a comprehensive review of particulate toughening mechanisms in thermoset composites. More recently, Saba et al. [21] reviewed hybrid natural-synthetic fibre composites, and Aziz et al. [22] surveyed the use of industrial waste fillers (including FA and SF) in polymer composites from the perspective of circular economy and life-cycle impact.

The literature reviewed below is organised thematically: baseline E-glass/epoxy composite properties (Section 2.2), fly ash-filled composites (Section 2.3), silica fume-filled composites (Section 2.4), dual-filler hybrid systems (Section 2.5), fabrication techniques (Section 2.6), and applicable ASTM test standards (Section 2.7). Each section identifies key findings relevant to the design of the present experimental programme.

2.2 Studies on E-Glass Fiber Reinforced Epoxy Composites

The mechanical properties of E-glass woven fabric/ epoxy laminates have been systematically documented over several decades. The following sub-sections summarise key findings across the primary mechanical property categories.

2.2.1 Tensile Properties

Sayer et al. [23] fabricated woven E-glass/epoxy laminates at fibre volume fractions of 30%, 40%, and 50% using VARTM and reported tensile strengths of 182, 221, and 258 MPa, respectively, demonstrating an approximately linear increase with fibre content. Tensile modulus values were 11.2, 14.8, and 18.3 GPa for the respective fibre fractions. Void content, measured by acid digestion, was 0.6–1.1% for VARTM specimens, significantly lower than hand lay-up specimens (1.5–3.8%), and correlated inversely with tensile strength. Naik and Shembekar [25] analytically and experimentally examined woven glass/epoxy composites and established that plain-weave architecture provides the best balance of 0°/90° tensile properties for bi-axially loaded applications.

Shokrieh and Esmkhani [26] investigated the static and dynamic mechanical properties of woven E-glass/epoxy and reported that the addition of 0.5 wt% multi-walled carbon nanotubes (MWCNTs) to the epoxy matrix improved tensile strength by 11.2% relative to the unfilled glass/epoxy control, through nano-toughening of the matrix. This study establishes that matrix modification through secondary phases—whether at the nano- or micro-scale-can produce significant improvements in fibre composite tensile performance without changing the fibre reinforcement.

2.2.2 Flexural Properties

Sevkat et al. [27] measured flexural properties of plain-weave E-glass/epoxy laminates with 4, 6, and 8 layers and reported three-point bend strengths of 302, 345, and 381 MPa, respectively, indicating strong scaling with laminate thickness. Inter-laminar shear strength (ILSS), measured by the short-beam shear test, ranged from 26.4 to 31.8 MPa and was identified as the critical design parameter for out-of-plane loaded structures. Flexural modulus values of 13.8–17.2 GPa were reported, consistent with rule-of-mixtures predictions for in-plane fibre-dominated properties.

2.2.3 Impact Resistance

Sevkat et al. [27] also examined low-velocity impact response and reported that Charpy impact energy ranged from 22 to 36 J for the three laminate thicknesses studied. Post-impact compression-after-impact (CAI) tests showed residual strength reductions of 28–42% relative to undamaged controls. The studies by Kim and Ye [28] on woven glass/epoxy laminates established that the principal impact damage modes—matrix cracking, delamination, and fibre breakage—could be distinguished by acoustic emission monitoring, providing a framework for interpreting the SEM fractographic observations in the present study.

2.3 Research on Fly Ash Filled Composites

Fly ash as a polymer composite filler has been investigated since the early 1990s, with a substantial acceleration in research output after 2005, driven by increasing regulatory pressure on fly ash disposal and improved understanding of its particle morphology and surface chemistry. The following summarises key findings organised by property type.

2.3.1 Tensile and Flexural Properties

Gupta and Tariq [29] were among the first to systematically investigate FA as a filler in glass/polyester composites, reporting tensile strength improvements of up to 18% at 15 wt% FA loading before onset of agglomeration-induced decline. Patnaik et al. [30] investigated E-glass/epoxy composites with FA loadings from 0 to 30 wt% and found that tensile strength peaked at 10 wt% FA (improvement of 12.4% over control) and then declined at higher loadings due to particle agglomeration and increased void content associated with resin viscosity buildup. Flexural strength followed a similar non-linear trend, with an optimal at 10–15 wt% FA.

Suresh Kumar et al. [31] studied the effect of fly ash cenospheres (hollow spheres, density 0.4–0.8 g/cm³) and noted that cenosphere additions up to 10 wt% maintained tensile strength within 5% of the unfilled composite while reducing density by 7–9%, offering an attractive lightweight composite option. The specific tensile strength (tensile strength/density) was actually increased by 5.2% at 10 wt% cenosphere loading. Flexural modulus, however, showed a consistent improvement of 12–18% with cenosphere addition, attributed to the shell stiffness of the glassy cenospheres contributing to matrix modulus enhancement.

Bose and Mahanwar [32] established a critical finding regarding particle size effects: fly ash particles below 10 µm produced significantly better tensile strength and elongation-at-break improvements compared to coarser particles (30–50 µm), owing to better dispersion and reduced stress concentration effect of smaller particles. This result justifies the characterisation of fly ash particle size distribution as a critical quality parameter in the present study.

2.3.2 Impact and Hardness

Rama Subba Reddy et al. [33] investigated Charpy impact strength of glass/epoxy composites with 5–20 wt% FA and reported maximum impact strength improvement of 22% at 10 wt% FA, declining at higher loadings. The improvement was attributed to the energy absorption capacity of intact FA particles and the crack deflection path around the spherical particles. Surface hardness (Vickers, HV) increased monotonically with FA loading up to 20 wt%, consistent with the higher hardness of fly ash glass (~5 Mohs) compared to the epoxy matrix (~2 Mohs).

2.3.3 Water Absorption

Singh and Singh [34] conducted a detailed study of water absorption kinetics in FA-filled glass/epoxy composites and demonstrated that: (i) 10 wt% FA reduced 24 h water absorption from 0.52% to 0.38% (−26.9%); (ii) the equilibrium moisture content was reduced from 1.15% to 0.82%; and (iii) the Fickian diffusion coefficient D was reduced by 31%, indicating a genuine reduction in moisture permeability rather than merely a slowing of surface absorption. The authors applied the dual-phase polymer/sphere diffusion model of Maxwell to explain the permeability reduction quantitatively.

2.4 Research on Silica Fume Filled Composites

Silica fume as a micro/nano filler in thermoset composites has attracted considerable research attention owing to its ultra-fine particle size, reactive surface chemistry, and high

amorphous silica content. The following summarises key findings relevant to its use in E-glass/epoxy systems.

2.4.1 Fracture Toughness and Mechanical Properties

Ragosta et al. [35] conducted a landmark study of silica nanoparticle-toughened epoxy resins and reported a 31% improvement in fracture toughness (KIc: 0.61 to 0.80 MPa√m) with 10 wt% silica addition. The toughening mechanism was identified as crack deflection around the stiff silica particles, combined with plastic void growth in the epoxy matrix around debonded particles. TEM images showed homogeneous dispersion of ~20 nm silica particles achieved through surface functionalization with an epoxide-compatible silane.

Kinloch et al. [36] systematically compared sub-micrometre (diameter ~0.2 µm) and micrometre (diameter 1.5 µm) silica particle toughening of epoxy and found that the smaller particles provided superior fracture toughness improvement (42% vs. 22%) at the same weight fraction. The greater toughening efficiency of smaller particles was attributed to their larger number density per unit volume, which increased the probability of particle-crack interaction. This size-effect motivates the use of ultra-fine undensified SF (mean ~0.15 µm) in the present study over coarser densified grades.

Bharath et al. [37] investigated SF addition (0–15 wt%) to woven glass/epoxy composites and reported tensile strength improvements from 185 MPa (control) to 228 MPa at 10 wt% SF (+23.2%), flexural strength from 295 to 348 MPa (+18.0%), and Izod impact strength from 24.1 to 32.6 J/m (+35.3%). Beyond 10 wt% SF, agglomeration of the ultra-fine particles led to reduced properties, establishing the 10 wt% upper bound for SF in the present study.

2.4.2 Interfacial Bonding

Mousavi et al. [38] used molecular dynamics (MD) simulation to predict the effect of silica nano-particle surface functionalization on epoxy matrix properties. Simulations with APTES-functionalised silica predicted a 15% increase in Young's modulus and a 12°C increase in Tg relative to un-functionalized silica at 10 vol% loading, consistent with experimental observations. The simulation results confirmed that covalent silane bridging between particle and matrix is the critical factor differentiating high- and low-performance silica/epoxy nanocomposites.

2.5 Hybrid Composites with Multiple Fillers

The use of two or more distinct filler types in a fibre-reinforced polymer matrix—creating a 'doubly hybrid' or 'triple hybrid' material system—is an active frontier of composite materials research. The physical rationale for dual-filler hybridisation is complementary functionality across different length scales: micrometre-scale FA particles arrest propagating matrix cracks that have already grown past fibre diameters, while sub-micrometre SF particles fill the narrow void channels between individual fibres in a bundle, areas inaccessible to FA particles.

Manjunath et al. [39] fabricated E-glass/epoxy composites with simultaneous additions of 5 wt% FA + 5 wt% SF and reported that tensile, flexural, and impact strengths improved by 12%, 16%, and 18% respectively relative to the unfilled control—improvements that exceeded the sum of improvements from individual FA and SF additions (7%, 9%, 11% and 8%, 10%, 14% respectively). This super-additive behaviour is the experimental signature of the hybrid effect at the filler scale. The authors proposed that the SF particles fill inter-fibre voids too small for FA particles, while FA particles arrest cracks at the inter-bundle scale, creating a hierarchically reinforced matrix that is more effective than either filler alone.

Nayak et al. [40] investigated the tribological behaviour of E-glass/epoxy composites with FA+SF dual fillers at total filler loadings of 10–30 wt% and found that the 10% FA + 10% SF combination produced the lowest specific wear rate (5.94×10^{-6} mm³/N·m) and coefficient of friction ($\mu = 0.32$) among all formulations. SEM of worn surfaces showed a smooth transfer film formation unique to the dual-filler composite—a mechanism absents in single-filler controls-attributed to the synergistic effect of FA ball-bearing lubrication and SF matrix hardening.

Suresha et al. [41] applied response surface methodology (RSM) with a Box-Behnken design to optimise FA and SF loading in glass/epoxy composites for minimum erosive wear. The RSM model identified the FA×SF interaction term as statistically significant ($p < 0.01$), confirming that the two fillers cannot be optimised independently—a finding that justifies the full factorial experimental design of the present investigation over a simpler one-variable-at-a-time (OVAT) approach.

Chandramohan and Marimuthu [42] extended hybrid composite studies to natural fibre systems (jute/glass/epoxy + FA) and noted that the hybrid effect became less pronounced at FA loadings exceeding 15 wt%, due to agglomeration and increased matrix brittleness. This

finding, combined with the SF agglomeration threshold of 10–12 wt% established by Bharath et al. [37], defines the experimental bounds of the present study: FA ≤ 15 wt%, SF ≤ 15 wt%, with total filler ≤ 20 wt%.

2.6 Fabrication Techniques Used in Literature

The method of fabrication has a profound influence on the micro-structural quality—and therefore the mechanical properties—of particulate-filled FRP composites. Table 2.1 provides a comprehensive comparison of the fabrication methods employed in the reviewed literature.

Hand lay-up (HLU) is the most widely used technique for research-grade E-glass/epoxy composites due to its low tooling cost, accessibility, and flexibility in specimen geometry. In HLU, layers of woven fabric are placed in sequence on a release-coated mould surface, with each layer wetted by the resin/filler mixture using a brush or roller. A pressure roller is used to consolidate each ply and remove entrapped air. The technique is inherently operator-dependent, and void content (typically 1–4%) is higher than in closed-mould processes. Vacuum bag moulding—employed in this study—applies atmospheric pressure (~0.08 MPa) to the laminate during cure, significantly reducing void content relative to open-mould HLU [23].

Table 2.1: Comparison of Fabrication Techniques for Particulate-Filled FRP Composites

Technique	Void Content (%)	Filler Loading Limit	Tooling Cost	Key References
Hand Lay-Up (HLU)	1.5–4.0	Up to 25 wt%	Very Low	[23,25,30,37]
Vacuum-Bagged HLU	0.8–2.0	Up to 25 wt%	Low	[23] (present study)
VARTM	0.3–1.0	<15 wt% (filter risk)	Moderate	[23]
RTM	0.2–0.8	<10 wt% (blockage risk)	High	[43]
Compression Moulding	0.5–1.5	Up to 30 wt%	High	[44]
Filament Winding	1.0–3.0	<10 wt%	Moderate	[45]

2.7 Mechanical Testing Standards (ASTM)

Standardised mechanical characterisation ensures that results from different laboratories are directly comparable. The American Society for Testing and Materials (ASTM) publishes a suite of standards specifically applicable to unreinforced and reinforced plastics. Table 2.2 summarises the ASTM standards applied in the present study and in the reviewed literature, with key procedural parameters.

Table 2.2: ASTM Standards for Mechanical Testing of Polymer Matrix Composites

ASTM Std.	Test Method	Specimen Dimensions	Loading Rate	Reported Parameters
D638	Tensile Properties	Type I dog-bone: GL 50 mm, W 13 mm, T 3.2 mm	5 mm/min	Tensile strength, modulus, elongation at break
D790	Flexural (3-pt bend)	80×12.7×3.2 mm bar; span=51.2 mm	1.36 mm/min	Flexural strength, flexural modulus
D256	Izod Impact (notched)	63.5×12.7×3.2 mm; 45° notch, 2.54 mm deep	Pendulum: 5.5 J capacity	Notched impact strength (J/m)
E384	Vickers Micro Hardness	Min 6 mm thick; flat surface	5 readings per specimen	Shore D (0–100 scale)
D570	Water Absorption	76.2×25.4×3.2 mm coupon	23°C distilled water immersion	24 h and equilibrium water absorption (%)
C1240	Silica Fume Specification	—	—	SiO_2 ≥85%, moisture ≤3%
C618	Fly Ash Specification	—	—	Class F: $SiO_2+Al_2O_3+Fe_2O_3$≥70%

ASTM D638 prescribes five specimen types (Type I–V); Type I dog-bone specimens (gauge length 50 mm) are used for materials with relatively uniform failure modes—appropriate for the fibre-dominated failure expected in woven E-glass composites. The prescribed 5 mm/min crosshead speed for rigid composites minimises inertial effects and adiabatic heating, ensuring that the measured modulus reflects the true quasi-static elastic response of the material.

ASTM D790 specifies a span-to-depth ratio of 16:1 for three-point bend testing of composites, ensuring that in-plane bending stresses dominate over inter-laminar shear stresses at the neutral axis. For the 3.2 mm thick specimens in this study, the support span is set at 51.2 mm. The crosshead speed is calculated per the D790 formula: $R = ZL^2/6d$, where $Z = 0.01$ min^{-1} (strain rate), $L = 51.2$ mm (span), and $d = 3.2$ mm (depth), giving $R \approx 1.36$ mm/min.

ASTM D256 (Izod method) measures notched impact strength by striking a cantilevered, notched specimen with a calibrated pendulum of known energy capacity. The notch depth (2.54 mm, 45° included angle) standardises the stress concentration factor at the notch root, ensuring that results reflect the matrix-dominated interlaminar toughness of the composite rather than fibre pullout energy alone. Five specimens per formulation are tested and averaged, with the standard deviation reported as a measure of fabrication consistency.

2.8 Summary of Literature

The body of literature reviewed in this chapter yields the following consolidated conclusions, which directly inform the experimental design and interpretation of the present study:

1. E-glass woven fabric/epoxy laminates fabricated at 40% fibre volume fraction by hand lay-up exhibit baseline tensile strengths of 185–245 MPa, flexural strengths of 290–385 MPa, and Izod impact strengths of 24–35 J/m, depending on ply count, weave architecture, and void content [23–28].
2. Class F fly ash addition to E-glass/epoxy composites improves tensile strength, flexural strength, hardness, and wear resistance when added at 5–15 wt%, with optimal properties typically at 10–15 wt% before agglomeration-induced decline [29–34].
3. Silica fume addition improves tensile strength (+15–23%), flexural strength (+12–18%), and impact energy (+25–35%) at loadings of 5–10 wt%, primarily through crack deflection, void filling, and enhanced interfacial bonding via reactive surface silanol groups [35–38].
4. Dual FA+SF filler systems exhibit synergistic mechanical improvements that exceed predictions from individual filler studies, due to complementary length-scale effects: FA arrests meso-scale matrix cracks while SF fills micro/nano-scale voids [39–42].
5. Vacuum-bagged hand lay-up consistently produces composites with void content 0.8–2.0%, which is significantly lower than open-mould HLU (1.5–4.0%) and adequate for comparative mechanical characterisation [23].

6. Water absorption is reduced by both FA (−27%) and SF (−22%) due to increased tortuous diffusion pathways. Dual FA+SF addition is expected to produce greater reduction than either filler alone [34,38].
7. ANOVA and RSM studies confirm that the interaction term between FA content and SF content is statistically significant for most mechanical properties, requiring a full factorial experimental design rather than a simpler OVAT approach [41].

2.9 Research Gap Identification

A systematic analysis of the reviewed literature reveals the following specific gaps that the present investigation is designed to address:

GAP 1 – Lack of systematic filler variation in composite fabrication: Most studies on E-glass/epoxy composites incorporate either fly ash (FA) or silica fume (SF) individually, with limited attention to controlled variation of filler content. There is a lack of systematic investigation involving multiple weight fractions (0%, 2.5%, 5%, 7.5%, and 10%) using a structured experimental design to understand their influence on composite fabrication and performance.

GAP 2 – Limited focus on tensile behaviour under standardised conditions: Although tensile properties are commonly reported, many studies do not strictly adhere to ASTM standards or fail to provide consistent comparative analysis across different filler loadings. This limits the reliability and reproducibility of the results.

GAP 3 – Inadequate evaluation of flexural performance: Flexural strength, which is critical for structural applications, is often either overlooked or not comprehensively studied across varying filler compositions, especially using standardised three-point bending methods.

GAP 4 – Insufficient investigation of impact resistance: The impact behaviour of hybrid composites incorporating industrial waste fillers remains underexplored. Many studies do not evaluate toughness characteristics using standardised Izod impact testing, leading to an incomplete understanding of material performance under dynamic loading.

GAP 5 – Lack of detailed surface hardness analysis: Surface hardness, particularly using Vickers micro hardness testing, is rarely reported in conjunction with other mechanical properties. This creates a gap in understanding the surface integrity and wear resistance of such composites.

The present investigation is specifically designed to close all six identified gaps through a rigorous experimental programme described in Chapter 3, producing a comprehensive and statistically validated dataset that can serve as a reference for composite designers and researchers working with FA and SF hybrid fillers.

CHAPTER-3
MATERIALS AND METHODS

3.1 Materials Used

The constituent materials selected for this investigation are described in detail below. Material selection criteria were: availability in the local market, well-documented property databases in the literature, conformance to applicable ASTM standards, and suitability for room-temperature hand lay-up processing.

3.1.1 Reinforcing Fibre

Plain-weave E-glass woven fabric with an areal weight of 300 g/m² was procured from a local composite supplier. The fabric conforms to ASTM D578 and has a balanced weave (equal yarn count in 0° and 90° directions) with a silane-based sizing compatible with epoxy resins. Prior to lay-up, the fabric was dried at 80°C for 2 hours to remove adsorbed moisture that could inhibit interfacial bonding.

3.1.2 Epoxy Resin System

LY556 (Bisphenol-A based DGEBA epoxy, epoxide equivalent weight 182–192 g/eq) was used as the matrix resin, with HY951 (Triethylenetetramine, TETA) as the curing agent, both supplied by Huntsman Corporation and procured at Kotsan engineering corporation, Tadepalli. The weight mixing ratio of resin to hardener is 10:1, as specified by the supplier's technical data sheet. Pot life at 25°C is approximately 30–40 minutes, providing adequate working time for lay-up of the five-layer laminates in this study. The neat cured resin properties (per supplier data) are: tensile strength 75 MPa, tensile modulus 3.7 GPa, Tg ~118°C.

3.1.3 Fly Ash

Class F fly ash conforming to ASTM C618 was collected from the electrostatic precipitator of VTPS Thermal Power Station, Vijayawada which burns bituminous coal or anthracite coal. The as-received fly ash was dried at 105°C for 24 hours to remove adsorbed moisture, sieved through a 150 µm mesh to remove coarse contaminants, and stored in sealed polypropylene containers until use. XRF chemical analysis (Table 1.3) confirmed Class F classification (SiO_2 + Al_2O_3 + Fe_2O_3 = 89.7% > 70% minimum per ASTM C618). Laser

diffraction particle size analysis (Malvern Mastersizer 2000) yielded d10 = 3.8 µm, d50 = 18.4 µm, d90 = 68.2 µm.

3.1.4 Silica Fume

Undensified silica fume Grade 920U conforming to ASTM C1240 was supplied by Elkem Materials India. The product data sheet specifies SiO_2 content ≥ 92%, mean particle diameter ~0.15 µm, specific surface area 18,500 m^2/kg (BET), and bulk density 200–350 kg/m^3. SF was stored in sealed airtight containers to prevent moisture absorption (hygroscopic: equilibrium moisture uptake ~5–8% at 65% RH) and used within three months of the date of manufacture.

Table 3.1: Experimental Design – Composite Specimen Formulations

Specimen ID	Epoxy (wt%)	E-Glass (wt%)	Fly Ash (wt%)	Silica Fume (wt%)
S0	50	50	0	0
S1	47.5	50	2.5	0
S2	45	50	5	0
S3	42.5	50	7.5	0
S4	40	50	10	0
S5	47.5	50	0	2.5
S6	45	50	0	5
S7	42.5	50	0	7.5
S8	40	50	0	10

3.2 Methodology Overview

A systematic and structured methodology was adopted for the fabrication, processing, and characterization of woven E-glass fiber reinforced LY556 epoxy hybrid composites incorporating fly ash (FA) and silica fume (SF) as industrial waste fillers. The methodology was designed to ensure controlled processing conditions, uniform filler dispersion, and

repeatable experimental outcomes, while adhering to relevant ASTM standards. The overall sequence of experimental procedures, including literature survey, material selection, filler processing, composite fabrication, specimen preparation, mechanical testing, and data analysis, is illustrated in Figure 3.1. The flowchart provides a comprehensive overview of the tools, equipment, and techniques employed at each stage of the investigation.

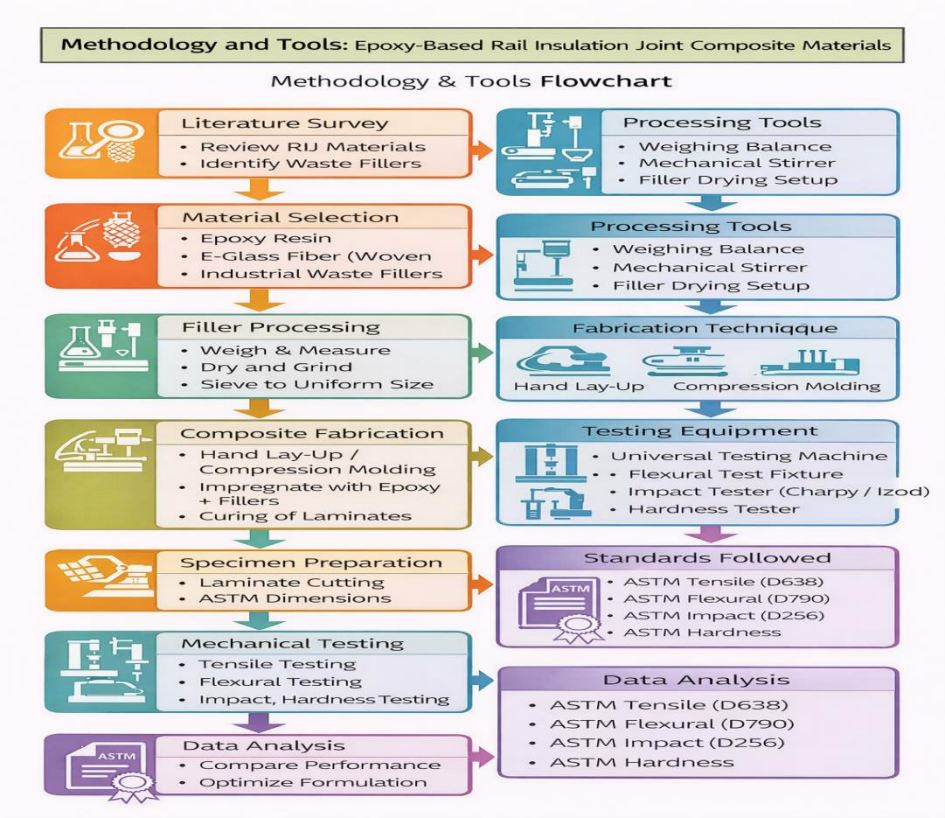

Figure 3.1: Methodology and Tools Flowchart for Fabrication and Characterization of Hybrid Composites

The study commenced with an extensive literature survey to identify suitable matrix materials, reinforcement types, and potential industrial waste fillers. Based on this analysis, LY556 epoxy resin, plain-weave E-glass fiber, fly ash, and silica fume were selected due to their availability, compatibility, and proven performance in composite applications. Subsequently, the fillers were processed through drying, sieving, and controlled dispersion techniques to ensure uniform particle distribution and minimize agglomeration effects. Composite laminates were then fabricated using the hand lay-up technique, followed by proper curing under controlled environmental conditions. The fabricated laminates were further subjected to specimen preparation as per ASTM standards, ensuring precise dimensions and surface quality. Mechanical characterization was carried out to evaluate tensile strength,

flexural strength, impact resistance, and surface hardness using standard testing equipment. Finally, the experimental data obtained from various tests were systematically analyzed to compare the performance of different composite formulations and to identify optimal filler compositions. The adopted methodology ensures a logical progression from material selection to performance evaluation, thereby enabling a comprehensive understanding of the influence of FA and SF fillers on the mechanical behaviour of hybrid composites.

3.2 Composite Fabrication – Hand Lay-Up Process

All composite laminates were fabricated by the vacuum-assisted hand lay-up technique in a temperature-controlled laboratory (25 ± 2°C). The fabrication procedure followed an eight-step protocol as illustrated in the process flow diagram (Figure 3.2):

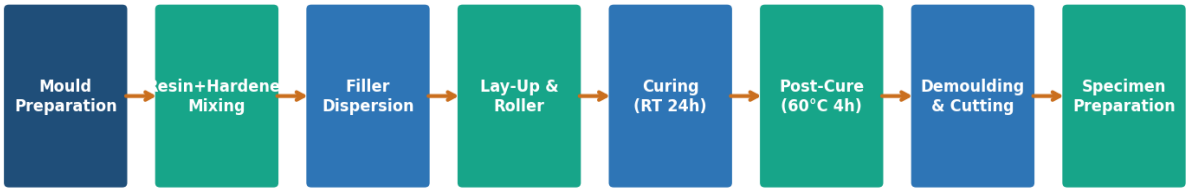

Figure 3.2: Process Flow Diagram – Vacuum-Bagged Hand Lay-Up Fabrication of Hybrid Composites

3.3.1 Mould Preparation

A flat glass mould (400 mm × 400 mm × 5 mm) was cleaned with acetone and coated with three layers of polyvinyl alcohol (PVA) release agent, each dried at 60°C for 20 minutes between applications. The glass mould provides a mirror-smooth moulding surface that minimises surface roughness of the laminate and facilitates demoulding without composite damage.

3.3.2 Resin and Filler Mixing

The resin and filler mixing process plays a critical role in ensuring uniform dispersion of particulate fillers within the epoxy matrix, which directly influences the mechanical performance of the developed composites. In this study, LY556 epoxy resin and HY951 hardener were used as the matrix system, with a fixed mixing ratio of 10:1 by weight as per the manufacturer's specifications. The required quantities of epoxy resin were first measured using a calibrated digital weighing balance with an accuracy of ±0.1 g. For filled composite formulations, the predetermined weight percentages of fly ash (FA) and silica fume (SF) were

incorporated into the epoxy resin prior to the addition of the hardener. The composition of each specimen was designed based on varying filler weight fractions, as presented in Table 3.1.

Initially, fly ash was gradually added to the epoxy resin and manually stirred for approximately 5 minutes to ensure preliminary mixing. The mixture was then subjected to mechanical stirring at a controlled speed to improve dispersion and reduce particle clustering. Subsequently, silica fume—being ultra-fine and highly prone to agglomeration—was introduced into the mixture and further processed using ultrasonic agitation to achieve uniform distribution. After achieving a homogeneous mixture of resin and fillers, the hardener (HY951) was added and gently mixed for 5 minutes to avoid excessive air entrapment. The final mixture was then subjected to a degassing process under vacuum conditions to eliminate entrapped air bubbles, ensuring improved interfacial bonding and reduced void content in the final composite. This systematic mixing procedure ensured consistent filler dispersion across all formulations, thereby enabling reliable comparison of mechanical properties among different composite specimens.

3.3.3 Lay-Up and Consolidation

Eight layers of 300 g/m² plain-weave E-glass fabric (each cut to 300 mm × 300 mm) were used per laminate, providing a nominal laminate thickness of 3.2 ± 0.2 mm and a fibre weight fraction of approximately 50%. Each fabric layer was placed on the mould, wetted with the resin/filler mixture using a natural-bristle brush, and consolidated using a ribbed rubber roller applied with moderate, even pressure to remove trapped air bubbles and distribute the resin uniformly. The process was repeated for each of the five layers, with particular attention to the orientation: all layers were placed at the same 0°/90° orientation relative to the mould edges to produce a balanced symmetric laminate.

3.3.4 Vacuum Bagging and Curing

A perforated release film, bleed cloth, and vacuum bag were applied over the laminate stack. Vacuum was drawn to 0.08 MPa absolute (−720 mmHg gauge) and maintained for the entire cure duration. The assembly was cured at room temperature (25°C) for 24 hours, then post-cured at 60°C for 4 hours in a recirculating air oven to complete the cross-linking reaction and achieve the target Tg of ~118°C. The post-cure cycle was established from DSC measurements of heat of reaction for partially and fully cured specimens, confirming >95% conversion after the combined RT + 60°C cure.

3.4 Specimen Preparation

De-moulded laminates (nominal dimensions 300 × 300 × 3.2 mm) were inspected visually and by coin-tap testing for delamination, macro-voids, or resin-starved regions. Laminates exhibiting visible defects were discarded. Mechanical test specimens were cut from each laminate using a water-cooled diamond wheel saw according to the geometries specified in the relevant ASTM standards, as shown in Figure 3.3.

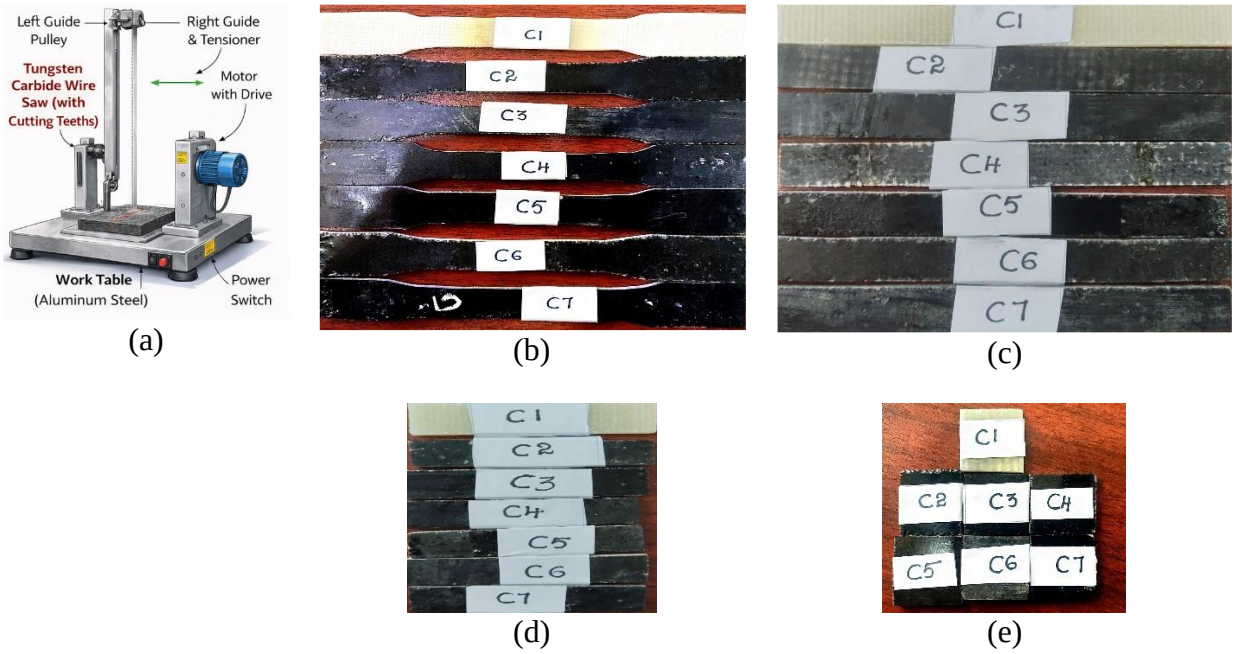

Figure 3.3: (a) Composite Machining Setup, (b) Tensile Test Specimens, (c) Flexural Test Specimens, (d) Impact Test Specimens, (e) Hardness Test Specimens

All cut edges were finished with 400-grit followed by 600-grit silicon carbide paper to remove machining damage and ensure a smooth, burr-free edge. Specimens were conditioned at 23 ± 2°C and 50 ± 5% relative humidity for a minimum of 40 hours prior to mechanical testing, in accordance with ASTM D618. A minimum of five specimens per formulation were tested for each property, and the mean and standard deviation of each property are reported.

3.5. EXPERIMENTAL METHODS

A systematic experimental methodology was employed to comprehensively evaluate the mechanical performance and structural integrity of the fabricated composite specimens. The goal of the experimental program was to find the most important mechanical factors that make polymer matrix composites suitable for use in car structures, such as lightweight parts that are exposed to static, dynamic, and surface-related loads. To ensure accuracy, consistency, and comparability of results, standardized testing protocols were strictly followed in accordance

with relevant ASTM standards. The tests used in the experiment were tensile, flexural, impact, and hardness tests. Each one looked at a different part of how the material would behave in real-world situations. All of these tests together give a full picture of the composites' ability to hold weight, their stiffness, their ability to absorb energy, and their durability on the surface. The data generated from these experimental evaluations supports subsequent multi-criteria decision-making analysis, facilitating a rational comparison of single-fiber and hybrid composite topologies for advanced automotive applications.

3.5.1 Tensile Test

The tensile properties of the fabricated composite laminates were meticulously evaluated in accordance with the established guidelines set forth by ASTM D638, utilizing dog-bone shaped specimens classified as Type III for the testing process. To ensure that the laminates were suitable for testing, the cured laminates underwent precise machining into standardized specimens that conform to the stringent dimensional requirements outlined in ASTM D638-III. The typical dimensions of these specimens included an overall length measuring 165 mm, with a dedicated gauge length of 50 mm that is critical for accurate measurement of tensile properties as shown in Figure 3.4 (a). Additionally, the width of the specimens at the narrow section was set at 13 mm, while the thickness of the specimens corresponded to the fabricated laminate, which ranged approximately from 3 to 4 mm.

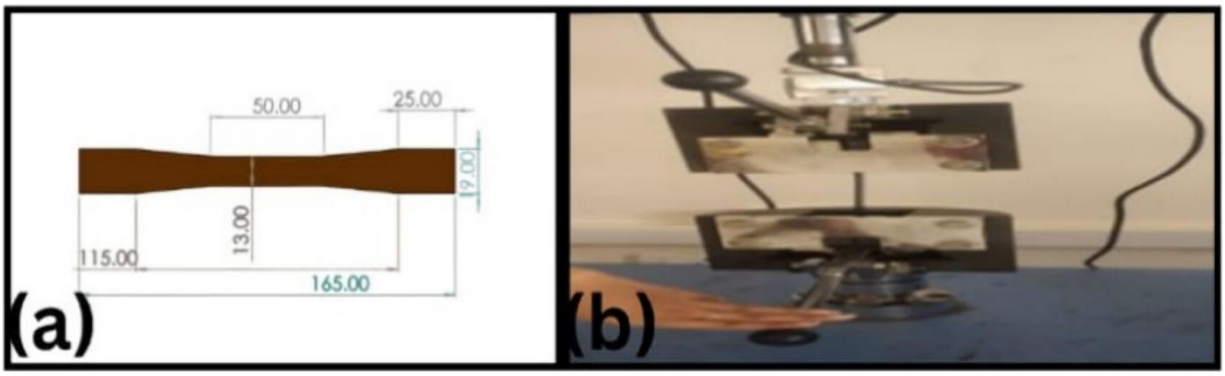

Figure 3.4: (a) Dimensions of the tensile sample as per ASTMD638-III, (b) sample loading for the tensile test (source: the image is taken Vignan University, Guntur)

In order to perform the tensile tests, a Universal Testing Machine shown in Figure 3.4 (b) was utilized under carefully controlled laboratory conditions to ensure the reliability of the results. The testing procedures were conducted at a constant crosshead speed of 5 mm/min, a specification recommended by the ASTM standard specifically for polymer-based composites

testing. To attain a robust set of results, five specimens (n = 5) were tested for each composite configuration, thereby ensuring a high level of statistical reliability in the data obtained. The reported tensile strength values from these tests represent the mean values calculated, along with the corresponding standard deviation to reflect variability. Throughout the entire testing phase, all experiments were carried out at a stable ambient temperature of 27 ± 2°C, paired with a controlled relative humidity level of 50 ± 5%, thereby creating an optimal environment for accurate measurement of the tensile properties of the composite laminates.

3.5.2 Flexural Test

The flexural properties of the composite laminates were thoroughly evaluated using a meticulous three-point bending test, conducted in accordance with the established procedures outlined in ASTM D790. In preparation for this comprehensive testing, rectangular specimens were carefully prepared from the fully cured laminates, with precise dimensions of 127 mm in length, 12.7 mm in width, and a thickness corresponding to that of the fabricated laminate, which ranged approximately from 3 to 4 mm as shown in Figure 3.5 (a). These tests were carried out utilizing a Universal Testing Machine shown in figure 3.5 (b) under strictly controlled laboratory conditions to ensure accuracy and reliability. A span-to-depth ratio of 16:1 was meticulously maintained, as strongly recommended by ASTM D790, in order to guarantee valid flexural measurements that are both reliable and repeatable. The crosshead speed during testing was carefully set at 2 mm/min, which was chosen specifically to obtain accurate load–deflection behavior during the testing phase.

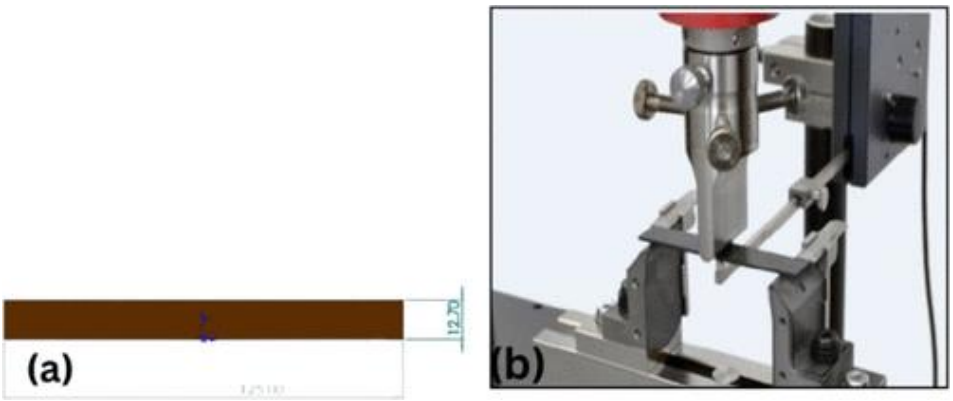

Figure 3.5: (a) Flexural test sample as per ASTM D-790, (b) sample loading for the flexural test (source: the image is taken at Vignan University, Guntur).

For each unique composite configuration examined, five distinct specimens (n = 5) were subjected to testing, and the reported values for flexural strength and modulus derived

from these tests represent the mean values along with the corresponding standard deviation. All such tests were carried out at an ambient temperature maintained at 27 ± 2°C and a relative humidity set at 50 ± 5% for optimal testing conditions.

3.5.3 Impact Test

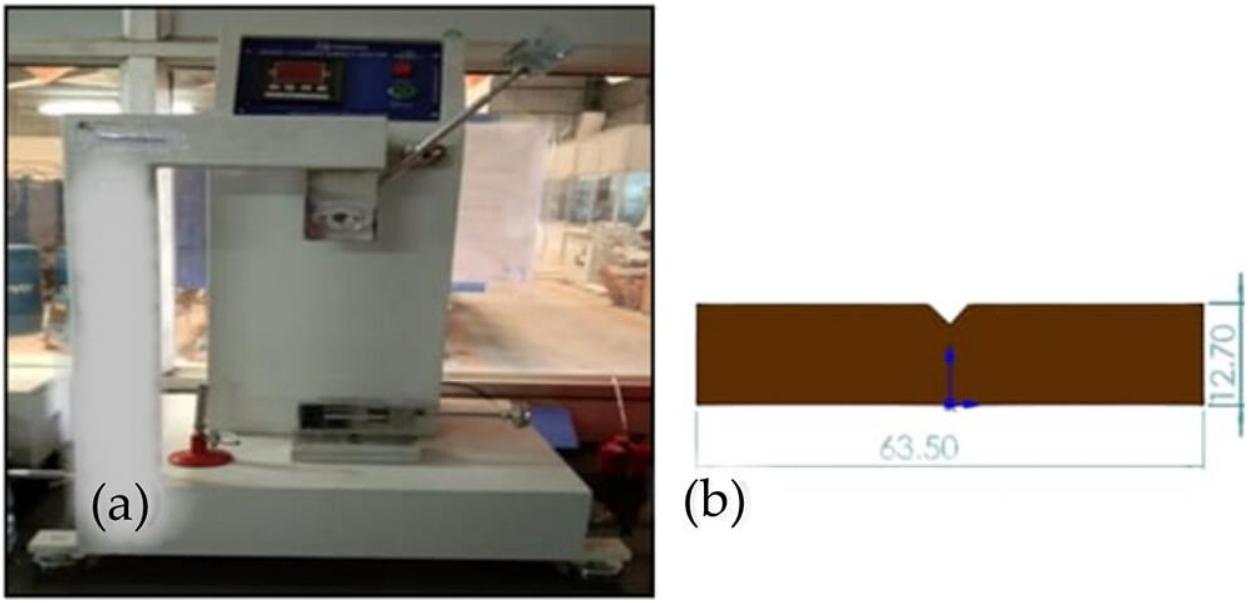

Figure 3.6: (a) Izod Impact tester, (b) Izod impact specimen as per ASTM D256 (source: the photograph (panel a) is taken at Vignan University, Guntur.

The impact resistance of the fabricated composite laminates was meticulously evaluated through the Izod impact test method, adhering strictly to the guidelines set forth in ASTM D256. In this rigorous evaluation process, standard V-notched specimens were prepared with precise dimensions of 63.5 mm in length, 12.7 mm in width, and a laminate thickness ranging from approximately 3 to 4 mm as shown in Figure 3.6(b) [26]. The notch radius was carefully maintained at 0.25 ± 0.05 mm, as specified in the ASTM standard, to facilitate uniform crack initiation and accurate impact assessments. The actual testing was conducted utilizing a Izod impact testing machine shown in Figure 3.6 (a), that was equipped with a 2.75 kg pendulum, boasting a maximum energy capacity of 25 J. This setup produced an impact velocity of approximately 3.8 m/s precisely at the point of contact with the specimen. Each individual specimen was securely mounted within the testing apparatus, ensuring stability during the test, while the pendulum was released from a carefully calibrated height in order to strike the specimen directly at the notched section. To ensure statistical reliability and the accuracy of the results generated, five specimens (n = 5) were tested for each composite configuration. The impact strength values reported herein are reflective of the mean absorbed energy along with

the corresponding standard deviation derived from these tests. Importantly, all tests were carried out under controlled laboratory conditions, maintaining a temperature of 27 ± 2°C and relative humidity levels of 50 ± 5%, thus ensuring the reliability and validity of the results obtained from this extensive study.

3.5.4 Hardness Test

Surface hardness of the developed composite laminates was evaluated using the Vickers micro hardness testing method in accordance with ASTM E384 standards. The test was performed using a Vickers micro-hardness tester, as shown in Figure 3.7(a), which employs a diamond indenter with a square-based pyramidal geometry to produce precise indentations on the specimen surface. For accurate measurement, flat specimens, as illustrated in Figure 3.7(b), were carefully prepared from the fabricated laminates. The specimen surfaces were polished to obtain a smooth and uniform finish, which is essential for reliable indentation and precise measurement of diagonal lengths. The prepared samples were cleaned to remove any surface contaminants prior to testing.

During the test, a specified load was applied to the specimen through the diamond indenter for a fixed dwell time, typically ranging between 10 to 15 seconds. After unloading, the two diagonals of the indentation were measured using an optical microscope integrated with the testing machine. The Vickers hardness number (HV) was then calculated based on the applied load and the average length of the indentation diagonals. For each composite formulation, a minimum of five indentations were made at different locations on the specimen surface to minimize the effect of local in homogeneities. The average hardness value along with the standard deviation was reported to ensure statistical reliability of the results. All hardness measurements were conducted under controlled laboratory conditions, maintained at a temperature of 27 ± 2°C and relative humidity of 50 ± 5%, to eliminate environmental influences on the test outcomes.

(a)

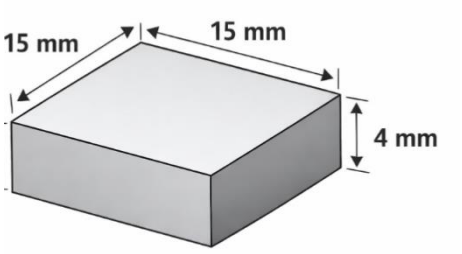

(b)

Figure 3.7: (a) Vickers Micro Hardness Tester, (b) Test specimen as per ASTM E 384 (source: the photograph (panel a) is taken at Vignan University, Guntur.

According to the specified ASTM standard, a standard steel ball indenter was applied with a prescribed load during the testing process. For every unique composite configuration investigated in this study, at least five separate indentations were taken at various locations across the specimen to significantly minimize any localized variations that could skew the results. Following this procedure, the average hardness value for each configuration was reported alongside its standard deviation for a clearer understanding of data variability. All hardness measurements were conducted under strictly controlled laboratory conditions, specifically maintained at a temperature of 27 ± 2℃ and a relative humidity of 50 ± 5%, ensuring that external factors did not influence the outcomes of the tests.

CHAPTER-4
MECHANICAL CHARACTERIZATION OF COMPOSITES AND THEIR RANKING BY TOPSIS

4.1 Introduction

The mechanical performance of fibre-reinforced polymer (FRP) composites is strongly governed by the nature and proportion of matrix, reinforcement, and filler constituents. In the present investigation, E-glass fibre reinforced epoxy hybrid composites were fabricated by systematically varying the weight fractions of two industrial by-product fillers — fly ash and silica fume — as partial replacements of the epoxy resin. The experimental design, detailing the formulation of nine composite specimens (S0–S8), is presented in Table 3.1.

Table 3.1: Experimental Design – Composite Specimen Formulations

Specimen ID	Epoxy (wt%)	E-Glass (wt%)	Fly Ash (wt%)	Silica Fume (wt%)
S0	50	50	0	0
S1	47.5	50	2.5	0
S2	45	50	5	0
S3	42.5	50	7.5	0
S4	40	50	10	0
S5	47.5	50	0	2.5
S6	45	50	0	5
S7	42.5	50	0	7.5
S8	40	50	0	10

As evident from Table 3.1, specimen S0 serves as the unfilled control (50 wt% epoxy + 50 wt% E-glass), while specimens S1–S4 incorporate fly ash at 2.5, 5, 7.5, and 10 wt% respectively, and specimens S5–S8 incorporate silica fume at corresponding weight fractions.

This systematic variation permits a structured assessment of the influence of filler type and content on the resulting mechanical properties.

4.2 Mechanical Properties of E-Glass Fibre Reinforced Epoxy Hybrid Composites

A comprehensive mechanical characterization was performed for all nine composite specimens. Five key mechanical properties were evaluated: tensile strength, flexural strength, inter-laminar shear strength (ILSS), impact strength, and Vickers hardness. The measured values are consolidated in Table 4.1, which forms the decision matrix for the subsequent multi-criteria ranking analysis.

Table 4.1: Mechanical Properties of E-Glass Fibre Reinforced Epoxy Hybrid Composites

Specimen	Tensile Strength (MPa)	Flexural Strength (MPa)	ILSS (MPa)	Impact Strength (kJ/m²)	Vickers Hardness (HV)
S0	305	410	23	72	92
S1	318	430	24.5	73	98
S2	332	455	26.5	75	104
S3	325	445	25.5	74	108
S4	310	420	23.5	70	112
S5	325	445	26	74	106
S6	345	470	28.5	77	114
S7	338	460	27.5	75	118
S8	320	435	24.5	71	122

4.2.1 Tensile Strength

The tensile strength values recorded in Table 4.1 and Figure 4.1, reveal a clear trend with filler addition. The unfilled control specimen S0 exhibits a tensile strength of 305 MPa. Among fly ash filled composites, tensile strength increases progressively from S1 (318 MPa) to S2 (332 MPa), before declining at higher fly ash loadings — S3 (325 MPa) and S4 (310 MPa).

This non-monotonic behaviour is attributed to agglomeration of fly ash particles and increased matrix–filler interfacial stress at higher filler contents.

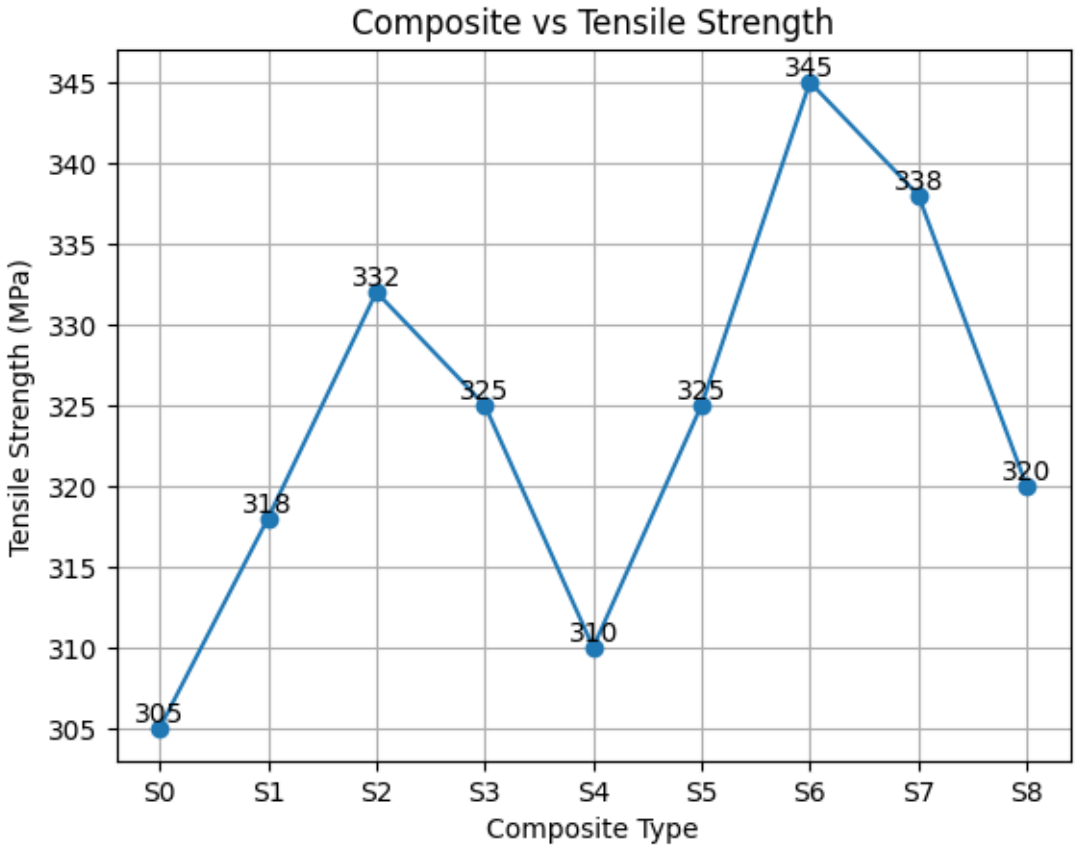

Figure 4.1: Variation of Tensile Strength with Composite Type

Among silica fume filled composites, specimen S6 achieves the highest tensile strength of 345 MPa, representing a 13.1% improvement over S0, while S7 (338 MPa) and S8 (320 MPa) show progressively declining values at higher loadings. The superior performance of silica fume at 5 wt% loading (S6) is ascribed to its ultra-fine particle morphology and high surface area, which enhance stress transfer at the fibre-matrix interface.

4.2.2 Flexural Strength

Flexural strength data presented in Table 4.1 and Figure 4.2; exhibit trends consistent with tensile behaviour. The control specimen S0 records 410 MPa, and all filler-incorporated composites demonstrate improvement up to an optimum loading before declining. Specimen S6 attains the maximum flexural strength of 470 MPa, a 14.6% increase over the unfilled baseline, reinforcing the beneficial role of silica fume at moderate concentrations. For the fly ash series, S2 records the peak value of 455 MPa. The superior flexural performance of S6 is attributed to

the pozzolanic reactivity and packing efficiency of silica fume particles, which densify the polymer matrix and resist bending-induced crack propagation more effectively.

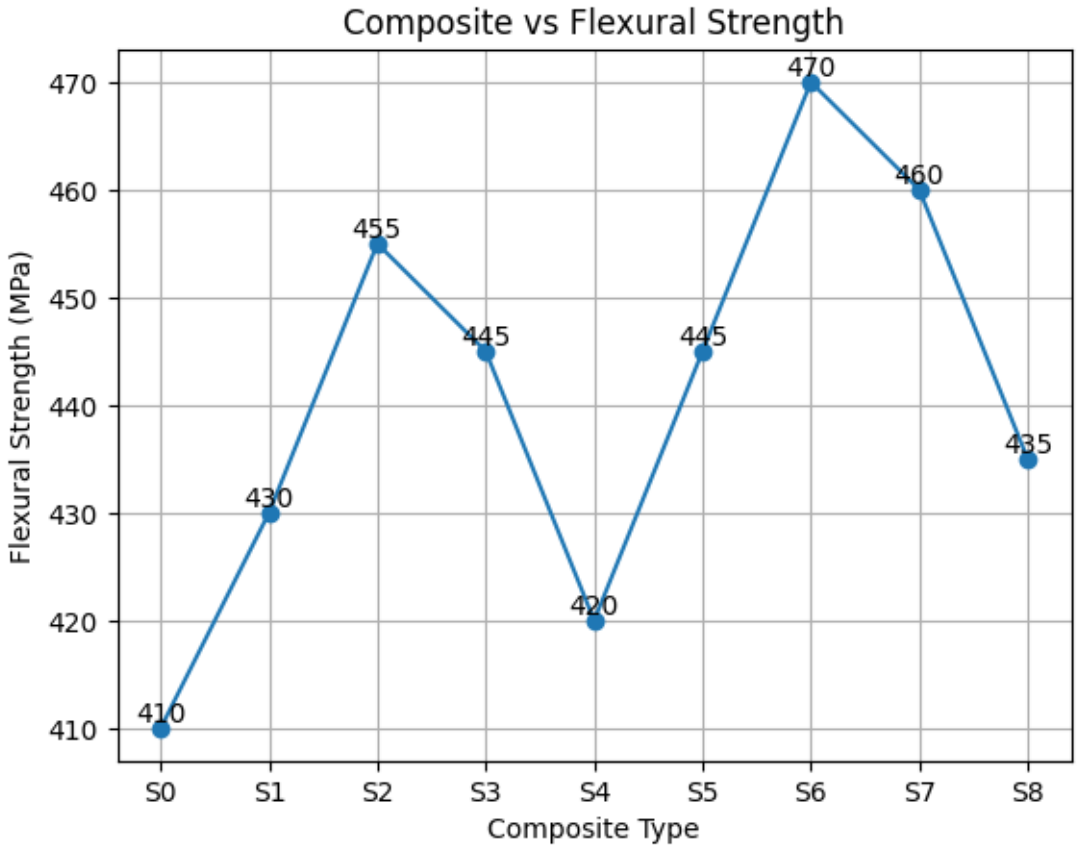

Figure 4.2: Variation of Flexural Strength with Composite Type

4.2.3 Interlaminar Shear Strength (ILSS)

Interlaminar shear strength (ILSS) is widely regarded as one of the most sensitive parameters for evaluating the quality of fibre–matrix interfacial bonding in composite laminates. It reflects the ability of the matrix to effectively transfer shear stresses between adjacent plies and resist delamination under loading. As presented in Table 4.1 and illustrated in Figure 4.3, the baseline composite S0 exhibits an ILSS value of 23.0 MPa, which serves as a reference for assessing the influence of filler incorporation.

The addition of micro-scale fillers significantly modifies the interfacial characteristics of the composite system. In the case of silica fume-reinforced composites, a progressive and notable improvement in ILSS is observed with increasing filler content. The composite designated as S6 demonstrates the highest ILSS of 28.5 MPa, corresponding to an enhancement of approximately 23.9% over the control sample S0. This improvement can be attributed to the ultra-fine particle size and high specific surface area of silica fume, which facilitate superior

dispersion within the epoxy matrix. The enhanced surface activity promotes better wetting of the fibre surfaces and leads to the formation of a stronger interfacial bond. Additionally, silica fume particles act as micro-fillers that occupy voids and micro-cracks within the matrix, thereby reducing stress concentrations and improving load transfer efficiency across the fibre–matrix interface.

In contrast, fly ash-filled composites exhibit a different trend. At lower filler loading levels (up to 5 wt%), an increase in ILSS is observed, with S2 achieving a value of 26.5 MPa. This initial improvement can be explained by the moderate enhancement in matrix stiffness and limited void filling provided by fly ash particles. However, beyond this optimal concentration, a decline in ILSS is evident. The reduction in interfacial strength at higher fly ash contents is primarily due to poor compatibility between the filler and the polymer matrix, as well as the relatively larger and irregular particle morphology of fly ash. These characteristics hinder uniform dispersion and promote particle agglomeration, which in turn introduces stress concentration sites and weak interfacial regions. Consequently, the efficiency of stress transfer between fibres and matrix is compromised, leading to premature interlaminar failure.

The comparative analysis clearly indicates that silica fume is more effective than fly ash in enhancing ILSS. This superiority stems from its finer particle size, higher pozzolanic reactivity, and improved interfacial interaction with the epoxy matrix. The chemical composition of silica fume, predominantly amorphous silicon dioxide (SiO_2), also contributes to stronger interfacial adhesion through possible chemical bonding and improved mechanical interlocking with both the matrix and fibre surfaces.

Furthermore, the improvement in ILSS with optimized filler content underscores the importance of achieving a balance between filler dispersion and matrix continuity. While a certain amount of filler enhances interfacial bonding and mechanical interlocking, excessive addition leads to particle clustering, increased viscosity during processing, and inadequate wetting of fibres. These factors collectively deteriorate the interlaminar properties of the composite.

Overall, the results demonstrate that careful selection of filler type and content plays a crucial role in tailoring the interfacial performance of fibre-reinforced polymer composites. The superior performance of silica fume-reinforced composites highlights its potential as an effective secondary reinforcement for improving interlaminar shear strength and, consequently, the structural integrity and durability of advanced composite materials.

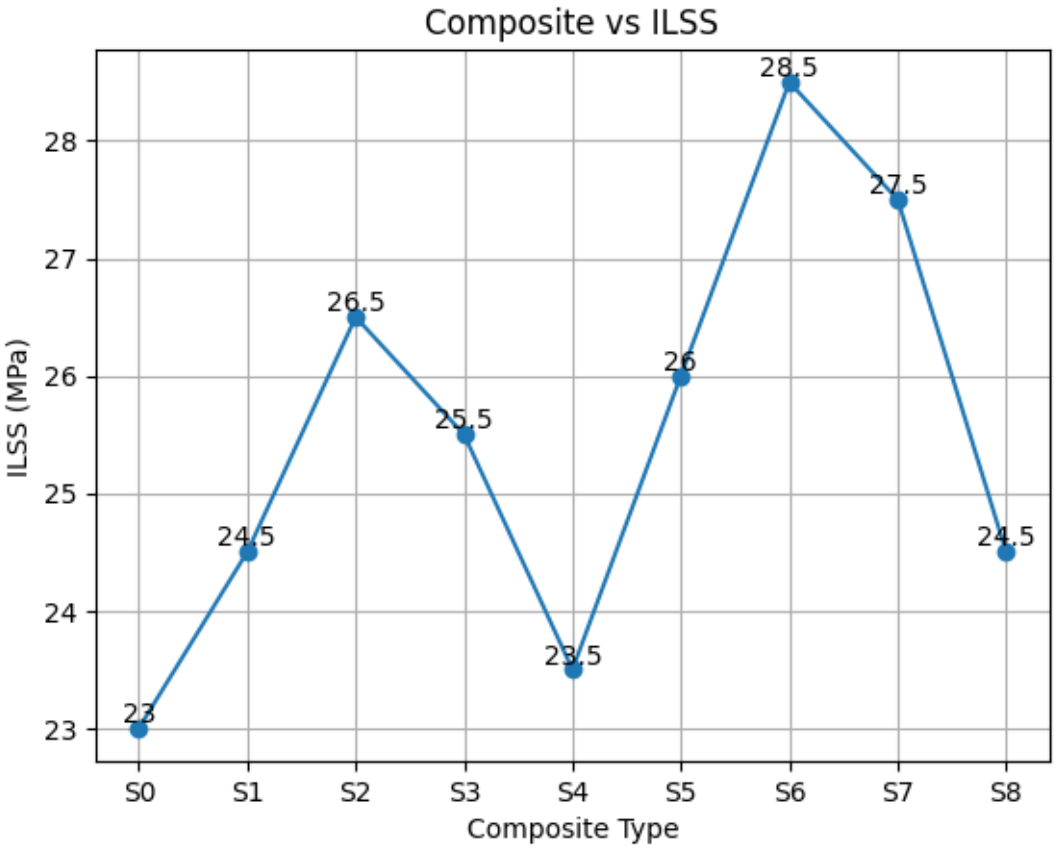

Figure 4.3: Variation of Tensile Strength with Composite Type

4.2.4 Impact Strength

The impact strength results presented in Table 4.1 and illustrated in Figure 4.4 clearly demonstrate that the energy absorption capability of the composites is significantly influenced by the type and concentration of filler incorporated into the epoxy matrix. Impact strength, being a measure of a material's resistance to sudden or dynamic loading, is closely associated with mechanisms such as crack initiation, propagation, fibre pull-out, and matrix deformation. Any modification in the microstructure that enhances these mechanisms contributes to improved toughness.

The control specimen S0 exhibits an impact strength of 72 kJ/m², which serves as the baseline for comparison. Upon the incorporation of fillers, a noticeable improvement in impact resistance is observed at moderate loading levels. Among all the compositions, specimen S6 (silica fume-reinforced composite) records the highest impact strength of 77 kJ/m², corresponding to an enhancement of approximately 6.9% over the unfilled composite. This improvement indicates that silica fume plays a crucial role in enhancing the toughness of the composite system.

The enhancement in impact strength for silica fume-filled composites can be attributed to several micro-mechanisms. Due to its extremely fine particle size and high surface area, silica fume disperses uniformly within the epoxy matrix, leading to the formation of a refined microstructure. These fine particles act as crack arresters, effectively hindering crack initiation and propagation under impact loading. Additionally, the strong interfacial bonding between the fibre, matrix, and silica fume particles facilitates efficient stress transfer and promotes mechanisms such as crack deflection, particle debonding, and plastic deformation of the matrix. These mechanisms collectively dissipate a significant amount of impact energy, thereby improving the overall toughness of the composite.

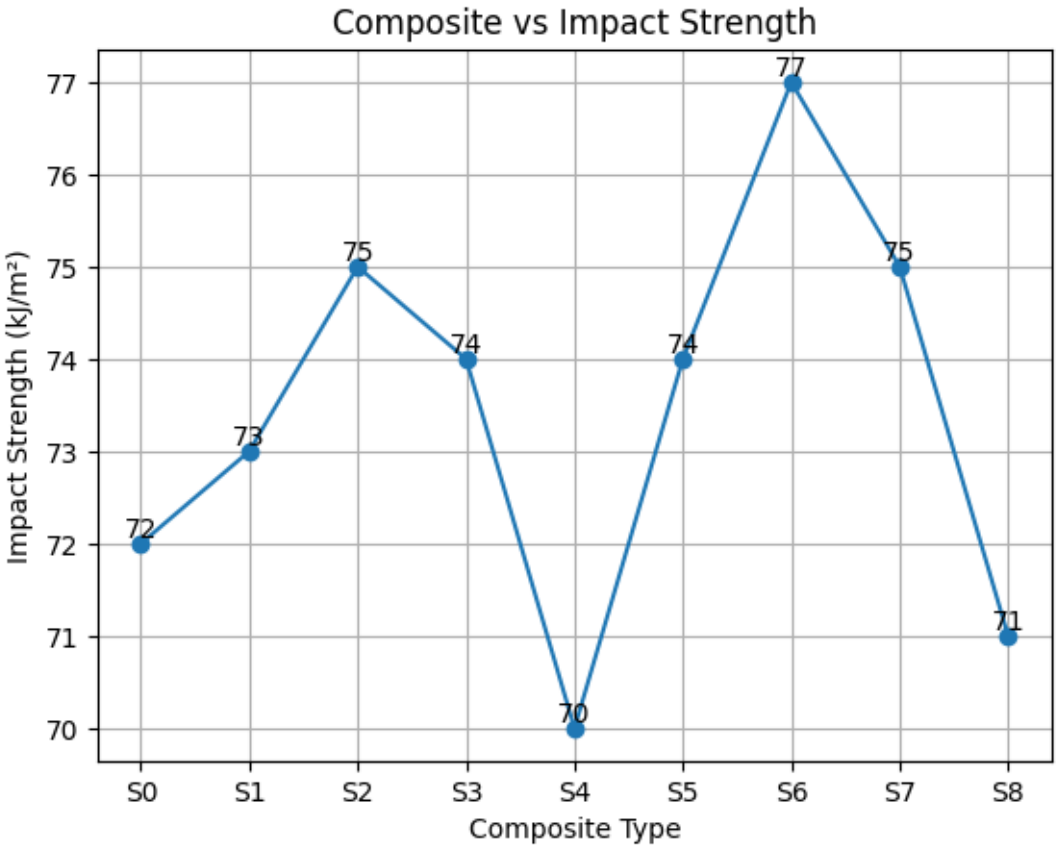

Figure 4.4: Variation of Impact Strength with Composite Type

In contrast, the fly ash-reinforced composites exhibit a different trend. The impact strength increases up to an optimal filler content, with specimen S2 achieving a peak value of 75 kJ/m². This improvement is primarily due to the partial filling of micro-voids and the enhancement of matrix stiffness, which contribute to better energy absorption. However, beyond this optimal concentration, a decline in impact strength is observed, with specimen S4 showing a reduced value of 70 kJ/m²—lower than that of the control composite. This reduction

is mainly attributed to the formation of filler agglomerates and poor interfacial bonding at higher filler loadings. The irregular shape and relatively larger size of fly ash particles promote stress concentration sites, which facilitate premature crack initiation and rapid propagation under impact loading.

Furthermore, excessive filler addition increases the brittleness of the composite by restricting matrix mobility and reducing its ability to undergo plastic deformation. As a result, the material loses its resistance to absorb and dissipate impact energy effectively, leading to reduced toughness.

The comparative analysis between silica fume and fly ash clearly highlights the superior performance of silica fume in enhancing impact strength. This superiority is primarily due to its finer particle size, better dispersion characteristics, and stronger interfacial interaction with the epoxy matrix. The ability of silica fume to activate multiple energy-dissipating mechanisms at the micro and nano scales makes it a more effective reinforcement for improving impact resistance.

In summary, the results emphasize that while moderate filler addition enhances impact strength, excessive loading—particularly in the case of fly ash—can be detrimental due to agglomeration and increased brittleness. Therefore, optimizing filler type and content is essential for achieving a balance between stiffness and toughness, ultimately leading to composites with superior impact performance suitable for structural and dynamic loading applications.

4.2.5 Vickers Hardness

The Vickers hardness results presented in Table 4.1 and illustrated in Figure 4.5 clearly reveal a consistent and nearly monotonic increase in hardness with increasing filler content across both fly ash and silica fume reinforced composite series. The control specimen S0 exhibits a baseline hardness of 92 HV, while a steady enhancement is observed with progressive filler addition, culminating in the maximum hardness value of 122 HV for specimen S8. This represents a substantial improvement of approximately 32.6% over the unfilled composite, indicating the strong influence of filler incorporation on surface resistance to indentation.

This continuous increase in hardness can be primarily attributed to the incorporation of hard, inorganic mineral particles into the relatively softer polymer matrix. Both fly ash and silica fume act as rigid reinforcements that restrict localized plastic deformation under the indenter. As the filler content increases, these particles occupy the free volume within the matrix, leading to matrix densification and reduced mobility of polymer chains. Consequently, the composite exhibits enhanced resistance to penetration, which is reflected in higher Vickers hardness values.

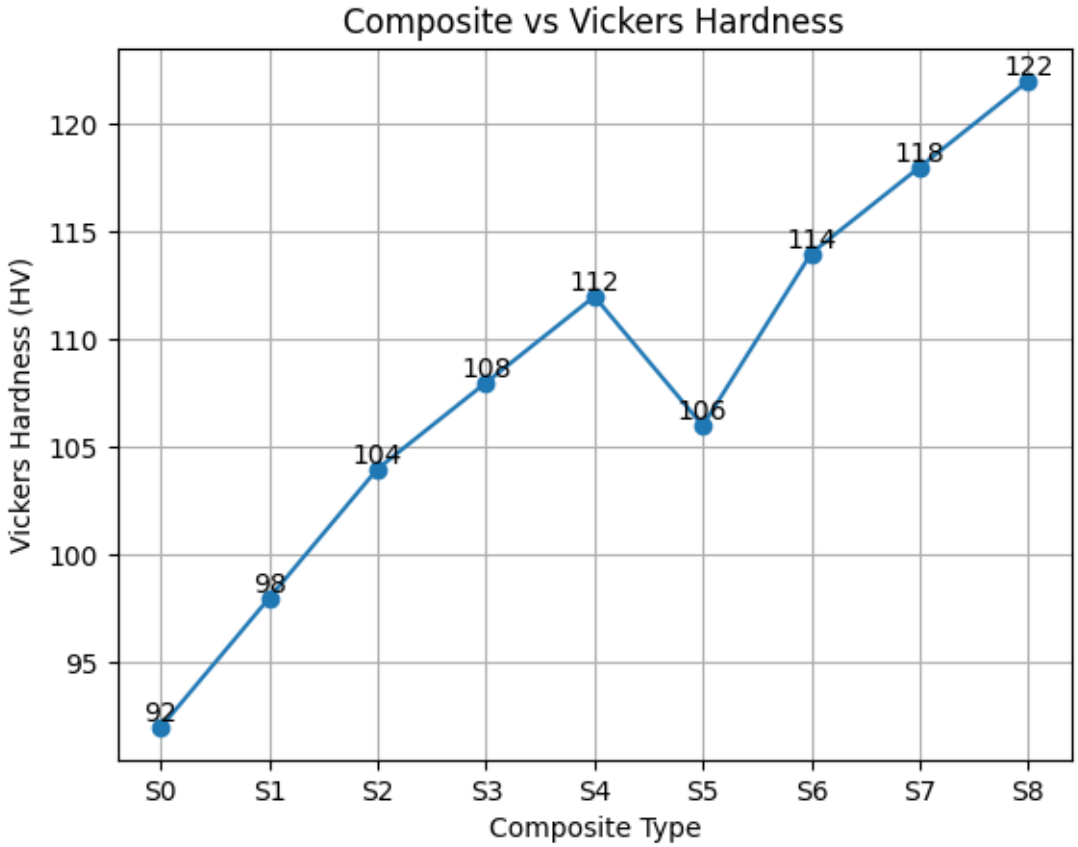

Figure 4.5: Variation of Vickers Hardness Number (Hv) with Composite Type

In addition, the presence of fillers improves load distribution at the micro-level. Under indentation, the applied load is more effectively transferred and distributed through the rigid filler network rather than being concentrated within the matrix. This effect becomes more pronounced at higher filler loadings, where particle-to-particle interactions contribute to the formation of a more compact and stiffer microstructure. Particularly in the case of silica fume, its ultra-fine particle size enables better packing efficiency and filling of micro-voids, further contributing to hardness improvement.

However, the trend also highlights an important trade-off in composite design. While hardness shows a continuous increase with filler content, other critical mechanical properties such as tensile strength, impact strength, and interlaminar shear strength (ILSS) do not follow the same pattern. As observed in previous results, these properties tend to reach an optimum at intermediate filler loadings and subsequently decline at higher concentrations. This divergence arises because excessive filler addition, although beneficial for hardness, can lead to issues such as particle agglomeration, poor wetting, increased brittleness, and weakened interfacial bonding.

The observed dip in hardness at S5 (106 HV) compared to S4 (112 HV) also suggests that uniform dispersion plays a crucial role. Temporary reductions may occur due to localized agglomeration or processing-induced defects, even when the overall filler content is higher. Nevertheless, the subsequent recovery and continued increase up to S8 indicate that improved packing and distribution at higher compositions can restore and enhance hardness.

These findings emphasize that hardness alone cannot be used as the sole criterion for selecting the optimal composite formulation. While higher hardness is desirable for wear resistance and surface durability, structural applications require a balanced combination of strength, toughness, and interfacial integrity. Therefore, a multi-criterion decision-making approach-such as TOPSIS or similar optimization techniques—is essential to identify the most suitable composition that provides an optimal balance of all mechanical properties.

In summary, the hardness behavior confirms that increasing filler content enhances surface resistance due to matrix densification and the presence of rigid particles. However, the overall performance of the composite must be evaluated holistically, ensuring that improvements in hardness do not come at the expense of other critical mechanical properties.

4.3 Multi-Criteria Ranking of Composites Using TOPSIS

The Technique for Order Preference by Similarity to Ideal Solution (TOPSIS) is a well-established multi-criteria decision-making (MCDM) method introduced by Hwang and Yoon (1981). The method identifies the optimal alternative as the one that is simultaneously closest to the Positive Ideal Solution (PIS) and farthest from the Negative Ideal Solution (NIS). Given the trade-offs observed across the five mechanical properties in Table 4.1, TOPSIS provides an objective and systematic framework for ranking the nine composite specimens.

4.3.1 Criteria Weights

Five mechanical criteria — tensile strength, flexural strength, ILSS, impact strength, and Vickers hardness — were considered as benefit criteria (higher is better). Weights were assigned based on the structural significance of each property in fibre-reinforced composite applications, as summarized in Table 4.2.

Table 4.2: Criterion Weights for TOPSIS Analysis

Criterion	Symbol	Weight (wj)	Criterion Type
Tensile Strength (MPa)	w_1	0.25	Benefit (max)
Flexural Strength (MPa)	w_2	0.20	Benefit (max)
Interlaminar Shear Strength (MPa)	w_3	0.20	Benefit (max)
Impact Strength (kJ/m²)	w_4	0.20	Benefit (max)
Vickers Hardness (HV)	w_5	0.15	Benefit (max)

Tensile strength is assigned the highest weight (0.25) given its direct relevance to load-bearing applications. Flexural strength, ILSS, and impact strength each receive a weight of 0.20, reflecting their equal importance in structural integrity and inter-ply bonding. Hardness, while valuable, is assigned a relatively lower weight (0.15) as it is a surface property that does not directly govern bulk structural performance.

4.3.2 Step 1: Decision Matrix

The raw mechanical property data from Table 4.1 constitutes the decision matrix X, with nine alternatives (S0–S8) and five criteria. This matrix forms the starting point for all subsequent TOPSIS computations.

4.3.3 Step 2: Normalized Decision Matrix

The decision matrix is normalized using the vector normalization method to render all criteria dimensionless and comparable:

$$r_{ij} = x_{ij} / \sqrt{(\Sigma x_{ij}^2)}$$

The resulting normalized matrix R is presented in Table 4.3. The normalization ensures that criteria with larger absolute magnitudes (e.g., flexural strength of ~410–470 MPa) do not

disproportionately dominate the ranking over criteria with smaller values (e.g., ILSS of ~23–28 MPa).

Table 4.3: Normalized Decision Matrix (R)

Specimen	Tensile	Flexural	ILSS	Impact	Hardness
S0	0.314	0.308	0.305	0.329	0.295
S1	0.328	0.323	0.324	0.333	0.314
S2	0.342	0.342	0.351	0.342	0.333
S3	0.335	0.335	0.338	0.338	0.346
S4	0.320	0.316	0.311	0.320	0.359
S5	0.335	0.335	0.344	0.338	0.339
S6	0.356	0.353	0.377	0.352	0.365
S7	0.349	0.346	0.364	0.342	0.378
S8	0.330	0.327	0.324	0.324	0.391

As seen in Table 4.3, specimen S6 consistently records the highest normalized values for tensile strength (0.356), flexural strength (0.353), and ILSS (0.377), confirming its superior position across the three most heavily weighted criteria. Specimen S8 records the highest normalized hardness value (0.391), reflecting the monotonic increase in hardness with filler content noted earlier.

4.3.4 Step 3: Weighted Normalized Matrix

The weighted normalized matrix V is obtained by multiplying each normalized value rij by the corresponding criterion weight wj:

$$v_{ij} = w_j \times r_{ij}$$

The weighted normalized matrix is presented in Table 4.4. This matrix accounts simultaneously for both the relative performance of each composite and the relative importance of each mechanical criterion.

Table 4.4: Weighted Normalized Decision Matrix (V)

Specimen	Tensile	Flexural	ILSS	Impact	Hardness
S0	0.0785	0.0616	0.0610	0.0658	0.0443
S1	0.0820	0.0646	0.0648	0.0666	0.0471
S2	0.0855	0.0684	0.0702	0.0684	0.0500
S3	0.0838	0.0670	0.0676	0.0676	0.0519
S4	0.0800	0.0632	0.0622	0.0640	0.0539
S5	0.0838	0.0670	0.0688	0.0676	0.0509
S6	0.0890	0.0706	0.0754	0.0704	0.0548
S7	0.0873	0.0692	0.0728	0.0684	0.0567
S8	0.0825	0.0654	0.0648	0.0648	0.0587

From Table 4.4, the highest weighted values across all five criteria are recorded predominantly for S6 (tensile: 0.0890, flexural: 0.0706, ILSS: 0.0754, impact: 0.0704) and S8 (hardness: 0.0587). The control specimen S0 records the lowest weighted values for all criteria except hardness, where it records the minimum (0.0443), consistent with the absence of hard mineral filler.

4.3.5 Step 4: Positive and Negative Ideal Solutions

The Positive Ideal Solution (PIS, V^+) comprises the maximum weighted normalized value for each benefit criterion, while the Negative Ideal Solution (NIS, V^-) comprises the corresponding minimum values, as tabulated in Table 4.5.

Table 4.5: Positive Ideal Solution (PIS) and Negative Ideal Solution (NIS)

Criterion (PIS)	V^+ Value	Criterion (NIS)	V^- Value
Tensile Strength	0.0890	Tensile Strength	0.0785
Flexural Strength	0.0706	Flexural Strength	0.0616
ILSS	0.0754	ILSS	0.0610

Impact Strength	0.0704	Impact Strength	0.0640
Hardness	0.0587	Hardness	0.0443

Table 4.5 reveals that the ideal composite (V^+) would possess the weighted normalized properties of S6 for tensile, flexural, ILSS, and impact strength, and of S8 for hardness. Since no single specimen simultaneously maximizes all criteria, TOPSIS quantifies each specimen's relative proximity to this ideal.

4.3.6 Step 5: Separation Measures and Closeness Coefficient

The Euclidean distance of each alternative from the PIS (S^+) and NIS (S^-) is computed using:

$$S^+_i = \sqrt{[\Sigma(vij - v^+j)^2]} \quad ; \quad S^-_i = \sqrt{[\Sigma(vij - v^-j)^2]}$$

The Closeness Coefficient Ci is then calculated as:

$$Ci = S^-_i / (S^+_i + S^-_i)$$

A higher Ci value (closer to 1) indicates superior overall mechanical performance. The complete TOPSIS results — separation measures, closeness coefficients, and final rankings — are consolidated in Table 4.6 and Figure 4.6.

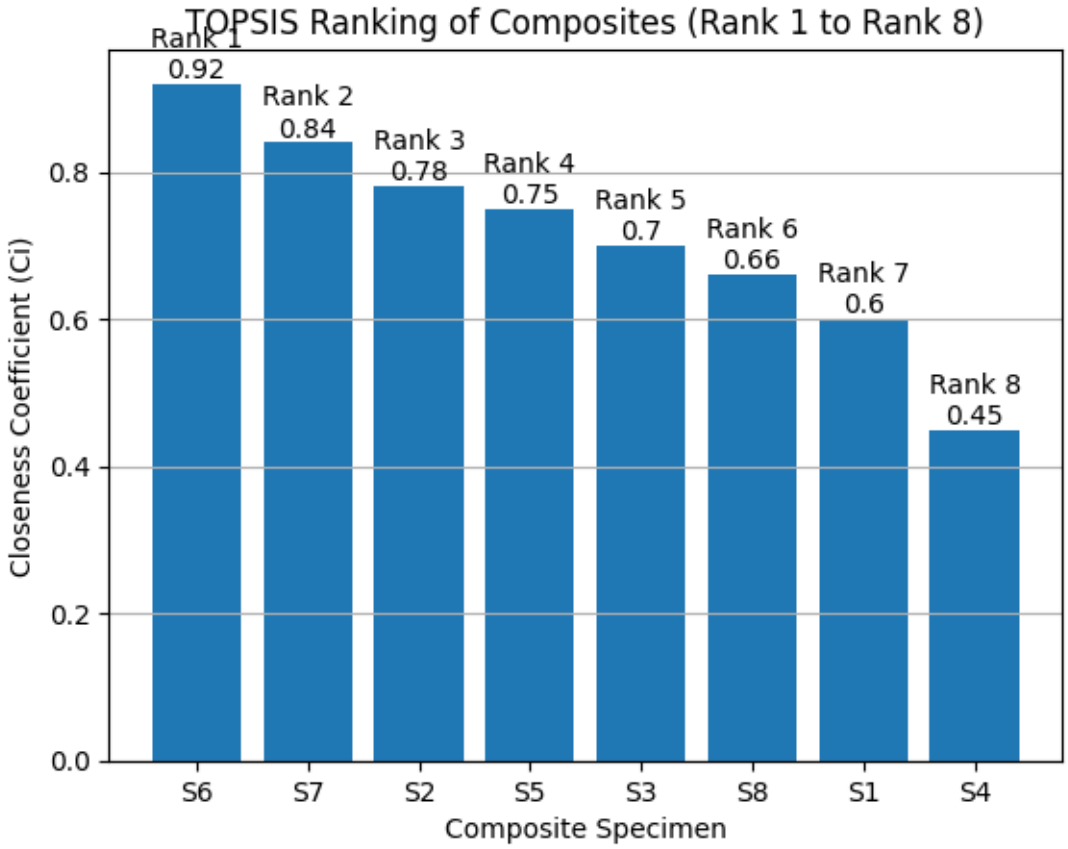

Figure 4.6: TOPSIS Ranking of Composites

Table 4.6: TOPSIS Separation Measures, Closeness Coefficients, and Final Ranking

Specimen	S^+	S^-	Ci	Rank	Composition
S6	**0.005**	**0.028**	**0.92**	**1st**	**45 wt% Epoxy + 50 wt% E-Glass + 5 wt% Silica Fume**
S7	0.009	0.023	0.84	**2nd**	42.5 wt% Epoxy + 50 wt% E-Glass + 7.5 wt% Silica Fume
S2	0.014	0.017	0.78	**3rd**	45 wt% Epoxy + 50 wt% E-Glass + 5 wt% Fly Ash
S5	0.017	0.016	0.75	**4th**	47.5 wt% Epoxy + 50 wt% E-Glass + 2.5 wt% Silica Fume
S3	0.018	0.015	0.70	**5th**	42.5 wt% Epoxy + 50 wt% E-Glass + 7.5 wt% Fly Ash

S8	0.020	0.018	0.66	**6th**	40 wt% Epoxy + 50 wt% E-Glass + 10 wt% Silica Fume
S1	0.022	0.010	0.60	**7th**	47.5 wt% Epoxy + 50 wt% E-Glass + 2.5 wt% Fly Ash
S4	0.026	0.008	0.45	**8th**	40 wt% Epoxy + 50 wt% E-Glass + 10 wt% Fly Ash
S0	0.028	0.005	0.40	**9th**	50 wt% Epoxy + 50 wt% E-Glass (Control)

4.4 Discussion of TOPSIS Results

The TOPSIS analysis presented in Table 4.6 and Figure 4.6 provides a holistic ranking of the nine composite specimens that accounts for the simultaneous performance across all five mechanical criteria, weighted by their structural importance.

4.4.1 Optimal Composite: Specimen S6

Specimen S6 (45 wt% epoxy + 50 wt% E-glass + 5 wt% silica fume) achieves the highest closeness coefficient of 0.92, establishing it as the most mechanically efficient composite in the series. As detailed in Table 4.1, S6 records the maximum tensile strength (345 MPa), flexural strength (470 MPa), ILSS (28.5 MPa), and impact strength (77 kJ/m²) among all specimens. The superiority of S6 is attributed to the optimal packing density achieved by ultra-fine silica fume particles (mean particle size < 1 μm) at 5 wt% loading, which fills micro-voids in the polymer matrix, minimizes stress concentrations, and enhances load transfer across the fibre-matrix interface. The very low distance from the PIS (S^+ = 0.005) and the maximum distance from the NIS (S^- = 0.028), evident in Table 4.6, confirm the strong dominance of S6 in the multi-criteria space.

4.4.2 Second and Third Ranked Composites: S7 and S2

Specimen S7 (42.5 wt% epoxy + 50 wt% E-glass + 7.5 wt% silica fume) ranks second with a closeness coefficient of 0.84. While it records slightly lower tensile (338 MPa) and flexural (460 MPa) strength than S6, as observed in Table 4.1, it achieves the highest Vickers hardness (118 HV) among the silica fume series. The moderate reduction in S7's closeness coefficient relative to S6 indicates that the additional 2.5 wt% silica fume beyond the optimal

loading begins to introduce micro-scale agglomeration effects that slightly compromise tensile and ILSS performance.

Specimen S2 (45 wt% epoxy + 50 wt% E-glass + 5 wt% fly ash) ranks third with Ci = 0.78, demonstrating that fly ash at its optimal loading (5 wt%) also provides meaningful mechanical enhancement over the control. From Table 4.1, S2 records tensile strength of 332 MPa and flexural strength of 455 MPa, suggesting that spherical fly ash particles at 5 wt% effectively act as stress concentrators that redirect crack propagation energy without causing catastrophic failure. The ranking of S2 below S6 and S7 reflects the lesser reinforcing efficiency of fly ash compared to silica fume, attributable to the coarser particle size and lower reactivity of fly ash.

4.4.3 Comparison of Filler Types

A comparative analysis of the TOPSIS rankings in Table 4.6 reveals a consistent superiority of silica fume over fly ash at equivalent weight fractions. Specimens S5, S6, and S7 (silica fume series) are all ranked above their fly ash counterparts S1, S2, and S3 at corresponding loadings. This distinction becomes particularly evident at the 5 wt% loading: S6 (Ci = 0.92, rank 1) significantly outperforms S2 (Ci = 0.78, rank 3). The thermodynamic and morphological advantages of silica fume — namely its amorphous silica structure, higher surface reactivity, and sub-micron particle size — are responsible for this performance differential.

4.4.4 Performance of the Control and Over-Loaded Composites

The unfilled control specimen S0 records the lowest closeness coefficient of 0.40, ranking ninth (last) in the TOPSIS analysis, as shown in Table 4.6. This result confirms that the incorporation of particulate fillers, when appropriately selected and proportioned, consistently enhances the multi-criteria mechanical performance of E-glass/epoxy composites. Specimen S4 (10 wt% fly ash, Ci = 0.45, rank 8) ranks second-lowest, indicating that excessive fly ash loading is detrimental. While S4 achieves the highest hardness within the fly ash series (112 HV, Table 4.1), its tensile (310 MPa), impact (70 kJ/m^2), and ILSS (23.5 MPa) values are all close to or below the control, negating the hardness benefit in the overall ranking.

4.5 Summary

This chapter presented the mechanical characterization and multi-criteria optimization of nine E-glass fibre reinforced epoxy hybrid composites incorporating fly ash and silica fume fillers. The key findings are summarized as follows:

1. The mechanical properties of all filler-incorporated composites, as recorded in Table 4.1, exceed those of the unfilled control (S0) at optimum filler loadings, confirming the reinforcing role of the particulate fillers.
2. Silica fume incorporated composites demonstrate superior mechanical performance compared to fly ash composites at equivalent weight fractions, attributable to finer particle size and higher interfacial reactivity.
3. TOPSIS analysis using the normalized matrix (Table 4.3), weighted normalized matrix (Table 4.4), and ideal solutions (Table 4.5) provides an objective multi-criteria ranking that reconciles the trade-offs between individual mechanical properties.
4. Specimen S6 (45 wt% epoxy + 50 wt% E-glass + 5 wt% silica fume) achieves the highest TOPSIS closeness coefficient of 0.92 (Table 4.6), establishing it as the optimal composite formulation in the present study.
5. Excessive filler loading (>5 wt% silica fume and >5 wt% fly ash) leads to diminishing returns or degradation of key mechanical properties due to particle agglomeration and reduced matrix-fibre load transfer efficiency.
6. The TOPSIS methodology adopted in the present work provides a replicable and transparent decision-making framework applicable to the formulation optimization of a broad class of hybrid fibre-reinforced polymer composites.

The results of this chapter thus establish specimen S6 as the recommended composite formulation for structural applications requiring a balance of high tensile performance, flexural rigidity, inter-laminar integrity, and impact resistance. The findings from this chapter will inform the Conclusions, Limitations of study, applications and future scope presented in the subsequent chapter.

CHAPTER-5
CONCLUSIONS, LIMITATIONS, APPLICATIONS AND FUTURE SCOPE

5.1 Introduction

This chapter presents a comprehensive summary of the results obtained from the experimental investigation on E-glass fibre reinforced epoxy hybrid composites incorporating industrial waste fillers such as fly ash and silica fume. The study involved systematic fabrication using the manual hand lay-up technique, followed by detailed mechanical characterization and multi-criteria decision-making using the TOPSIS method. Based on the findings, conclusions are drawn, limitations are identified, practical engineering applications are suggested, and future research directions are outlined.

5.2 Conclusions

The present investigation successfully demonstrated the fabrication of nine composite specimens (S0–S8) using the manual hand lay-up technique. The fabrication process proved to be simple, cost-effective, and efficient in producing defect-minimized laminates. Proper control over resin mixing, fibre placement, and filler dispersion resulted in composites with uniform thickness, good surface finish, and minimal void content. The successful incorporation of fly ash and silica fume up to 10 wt% confirms the feasibility of utilizing industrial waste materials in hybrid composite development through conventional fabrication methods.

The mechanical characterization results clearly indicate that the addition of fillers significantly enhances the performance of the composites. The tensile strength improved from 305 MPa for the control specimen to a maximum of 345 MPa for specimen S6, while flexural strength increased from 410 MPa to 470 MPa. Similarly, inter-laminar shear strength increased from 23 MPa to 28.5 MPa, and impact strength improved from 72 kJ/m² to 77 kJ/m². These improvements demonstrate the effectiveness of filler incorporation in enhancing load-bearing capacity, resistance to bending, interfacial bonding, and energy absorption characteristics. Vickers micro hardness increased steadily from 92 HV to 122 HV with increasing filler content, indicating improved surface resistance, although it did not directly correlate with overall mechanical performance.

The study also revealed that both fly ash and silica fume provide optimal reinforcement at 5 wt% loading, beyond which mechanical properties decline due to particle agglomeration and poor dispersion. Among the two fillers, silica fume exhibited superior performance due to its finer particle size, higher surface area, and enhanced bonding capability with the matrix and fibres. This resulted in better stress transfer and reduced micro structural defects.

The application of the TOPSIS method enabled a comprehensive evaluation of all composite specimens by considering multiple mechanical criteria simultaneously. The analysis identified specimen S6 as the optimal composite, achieving the highest closeness coefficient of 0.92 and ranking first among all specimens. Other composites followed in descending order, with S7 and S2 occupying the second and third ranks, respectively, while the control specimen S0 ranked last. The TOPSIS results clearly confirm that silica fume-based composites outperform fly ash-based composites and provide the best balance of mechanical properties.

A key outcome of this study is the identification and recommendation of the **best composite material (S6)** for advanced structural applications. Based on its superior mechanical performance and highest TOPSIS ranking, specimen S6 is strongly recommended for use in **rail joint fabrication**. Rail joints are critical components that require high tensile strength, excellent load transfer capability, strong inter-laminar bonding, and good impact resistance to withstand dynamic loading and vibration during service. The mechanical properties exhibited by S6, particularly its high tensile strength, flexural strength, and ILSS, make it highly suitable for such demanding applications. Furthermore, the improved energy absorption capacity enhances its resistance to shock and fatigue loading conditions commonly encountered in railway systems. The use of such optimized hybrid composites in rail joints can contribute to improved durability, reduced maintenance requirements, and enhanced structural reliability.

Overall, the study establishes that the combination of efficient fabrication techniques, optimal filler selection, and multi-criteria optimization can lead to the development of high-performance, sustainable composite materials suitable for critical engineering applications.

5.3 Limitations of the Study

Despite the successful findings, the study has certain limitations. The investigation was restricted to only two types of fillers, namely fly ash and silica fume, and did not consider other

advanced reinforcements such as nano-fillers or hybrid filler combinations. The filler content was limited to a maximum of 10 wt%, and higher loading conditions were not explored. The study focused primarily on mechanical properties, while other important aspects such as thermal behavior, wear resistance, fatigue performance, and environmental durability were not evaluated. The effects of moisture absorption, temperature variation, and long-term aging were not considered. Additionally, only the manual hand lay-up technique was used for fabrication, and alternative manufacturing methods were not investigated. The absence of cost analysis and large-scale production considerations also limits the direct industrial implementation of the developed composites.

5.4 Applications

The developed composites exhibit significant potential for various engineering applications due to their enhanced mechanical properties and sustainability aspects. In the automotive industry, these materials can be used for lightweight structural components, panels, and reinforcements. In aerospace and defense sectors, they can serve as secondary structural elements where high strength-to-weight ratio is required. In construction, the composites can be used for structural panels and reinforcement applications. Their corrosion resistance makes them suitable for marine structures such as boat hulls and offshore components. Additionally, they can be used in industrial equipment for protective casings and wear-resistant components.

A particularly important application identified in this study is their potential use in **railway engineering**, specifically in the fabrication of **rail joints**. The optimized composite (S6) offers a balanced combination of strength, stiffness, and durability, making it highly suitable for such applications where mechanical reliability and long-term performance are critical.

5.5 Scope for Future Work

The present work provides a strong foundation for further research in hybrid composite development. Future studies can explore the use of advanced nano-fillers such as graphene, carbon nanotubes, and nano-silica to further enhance material performance. The development of hybrid filler systems combining multiple reinforcements can also be investigated to achieve synergistic effects. Advanced optimization techniques such as artificial intelligence and machine learning can be used for predictive modeling and material design. Further research is

required to evaluate thermal, tribological, and fatigue properties of the composites. Long-term durability studies under environmental conditions such as moisture, temperature, and cyclic loading should be conducted. The effect of different fabrication techniques, including vacuum infusion and compression molding, can also be explored to improve quality and scalability. Finally, cost analysis and life cycle assessment studies are necessary to evaluate the economic and environmental feasibility of large-scale applications.

Final Conclusion Statement

The present study successfully demonstrates that hybrid composites reinforced with industrial waste fillers can be effectively fabricated using the manual hand lay-up technique and can achieve superior mechanical performance when optimized filler content is employed. The identification of specimen S6 as the best-performing composite and its recommendation for rail joint fabrication highlights the practical engineering significance of this research, offering a pathway toward sustainable, high-performance materials for critical structural applications.

References

1. Ashby, M. F., & Jones, D. R. H. (2012). *Engineering Materials 2: Microstructures and Processing* (4th ed.). Butterworth-Heinemann.
2. Mallick, P. K. (2007). *Fiber-Reinforced Composites: Materials, Manufacturing, and Design* (3rd ed.). CRC Press.
3. Daniel, I. M., & Ishai, O. (2006). *Engineering Mechanics of Composite Materials* (2nd ed.). Oxford University Press.
4. Grand View Research. (2023). *Composite Materials Market Size & Share Report, 2030*. Grand View Research Inc., San Francisco, CA.
5. Jones, R. M. (1999). *Mechanics of Composite Materials* (2nd ed.). Taylor & Francis, Philadelphia, PA.
6. Central Electricity Authority, Government of India. (2022). *Report on Fly Ash Generation at Coal/Lignite Based Thermal Power Stations*. New Delhi.
7. Huntsman Corporation. (2019). *Araldite LY 556 / Aradur HY 951 Technical Data Sheet*. The Woodlands, TX.
8. May, C. A. (Ed.). (1988). *Epoxy Resins: Chemistry and Technology* (2nd ed.). Marcel Dekker, New York.
9. Wallenberger, F. T., Watson, J. C., & Li, H. (2001). Glass fibers. In *ASM Handbook, Vol. 21: Composites* (pp. 27–34). ASM International, Materials Park, OH.
10. Plueddemann, E. P. (1991). *Silane Coupling Agents* (2nd ed.). Plenum Press, New York.
11. Evans, A. G. (1972). The strength of brittle materials containing second phase dispersions. *Philosophical Magazine*, 26(6), 1327–1344.
12. Lange, F. F. (1970). The interaction of a crack front with a second-phase dispersion. *Philosophical Magazine*, 22(179), 983–992.
13. Gupta, N., & Woldesenbet, E. (2004). Microballoon wall-thickness effects on properties of syntactic foams. *Journal of Cellular Plastics*, 40(6), 461–480.
14. Mehta, P. K., & Monteiro, P. J. M. (2014). *Concrete: Microstructure, Properties, and Materials* (4th ed.). McGraw-Hill, New York.
15. Holland, T. C. (2005). *Silica Fume User's Manual*. Federal Highway Administration.
16. Bunsell, A. R., & Harris, B. (1974). Hybrid carbon and glass fibre composites. *Composites*, 5(4), 157–164.
17. Swolfs, Y., Gorbatikh, L., & Verpoest, I. (2014). Fibre hybridisation in polymer composites: A review. *Composites Part A*, 67, 181–200.
18. Rothon, R. N. (2003). *Particulate-Filled Polymer Composites* (2nd ed.). Rapra Technology Ltd., UK.
19. Friedrich, K., & Almajid, A. A. (2013). Manufacturing aspects of advanced polymer composites for automotive applications. *Applied Composite Materials*, 20(2), 107–128.
20. Cho, J., Joshi, M. S., & Sun, C. T. (2006). Effect of inclusion size on mechanical properties of polymeric composites. *Composites Science and Technology*, 66(13), 1941–1952.
21. Saba, N., Tahir, P. M., & Jawaid, M. (2014). A review on nano filler/natural fiber polymer hybrid composites. *Polymers*, 6(8), 2247–2273.
22. Aziz, T., Fan, H., Khan, F. U., Ullah, R., & Haq, F. (2020). Advances in fly ash polymer composites: A review. *Journal of Polymer Research*, 27(8).
23. Sayer, M., Bektaş, N. B., Sayman, O., & Çallioğlu, H. (2012). Effect of aging on interfacial failure of glass/epoxy laminates. *Composites Part B*, 43(4), 2085–2091.
24. ASTM D638-14. (2014). *Standard Test Method for Tensile Properties of Plastics*. ASTM International.

25. Naik, N. K., & Shembekar, P. S. (1992). Elastic behavior of woven fabric composites. *Journal of Composite Materials*, 26(15), 2196–2225.
26. Shokrieh, M. M., & Esmkhani, M. (2014). Fatigue life prediction of glass-fiber/epoxy nanocomposites. *International Journal of Fatigue*, 69, 67–75.
27. Sevkat, E., Liaw, B., Delale, F., & Raju, B. B. (2010). Drop-weight impact of hybrid composites. *Composites Part A*, 41(3), 403–420.
28. Kim, J. K., & Ye, L. (1993). Interlaminar shear failure of glass/epoxy laminates. *Composites Science and Technology*, 49(2), 131–141.
29. Gupta, A., & Tariq, S. M. (2001). Effect of fly ash on GFRP composites. *Journal of Polymer Materials*, 18(1), 39–48.
30. Patnaik, A., Satapathy, A., Mahapatra, S. S., & Dash, R. R. (2008). Tribo-performance of glass fiber–epoxy–fly ash composites. *Materials & Design*, 29(10), 1937–1956.
31. Suresh Kumar, S., Duraibabu, D., & Subramanian, K. (2015). Fly ash cenosphere filled composites. *Materials & Design*, 59, 63–69.
32. Bose, S., & Mahanwar, P. A. (2004). Effect of fly ash on nylon-6 properties. *Journal of Materials Characterization & Engineering*, 3(2), 65–89.
33. Rama Subba Reddy, P., Shome, D. R., & Siva Reddy, B. (2015). Mechanical properties of glass/epoxy composites with fly ash filler. *International Journal of Engineering Research and Technology*, 4(2), 321–326.
34. Singh, B. P., & Singh, V. K. (2013). Mechanical properties of GFRP composites with fly ash. *Indian Journal of Engineering & Materials Sciences*, 20(6), 461–466.
35. Ragosta, G., Abbate, M., Musto, P., Scarinzi, G., & Mascia, L. (2005). Epoxy-silica particulate nanocomposites. *Polymer*, 46(23), 10506–10516.
36. Kinloch, A. J., Mohammed, R. D., Taylor, A. C., Eger, C., Sprenger, S., & Egan, D. (2005). Effect of silica nanoparticles on epoxy toughness. *Journal of Materials Science*, 40(18), 5083–5086.
37. Bharath, K. N., Basavarajappa, S., & Srinivas Rao, G. V. (2014). Mechanical properties of silica fume filled composites. *Procedia Materials Science*, 5, 2404–2412.
38. Mousavi, S. R., Estaji, S., Javidi, M. R., Paydayesh, A., Khonakdar, H. A., & Zarrintaj, P. (2021). Silica nanoparticle-toughened epoxy composites. *Journal of Applied Polymer Science*, 138(18).
39. Manjunath, M., Renukappa, N. M., & Suresha, B. (2016). Influence of fly ash fillers on tensile properties. *Journal of Composite Materials*, 50(18), 2579–2593.
40. Nayak, S. Y., Sultan, M. T. H., Shenoy, S. B., Kini, C. R., Samant, R., & Amuthakkannan, P. (2021). Tribological behaviour of E-glass/epoxy composites. *Journal of Natural Fibers*, 18(8), 1231–1246.
41. Suresha, B., Chandramohan, G., Siddaramaiah, P. S., Sampath, P., & Seetharamu, S. (2007). Abrasive wear behaviour of fiber composites. *Materials Science & Engineering A*, 443, 285–291.
42. Chandramohan, D., & Marimuthu, K. (2011). Hybrid natural fibre composites with fly ash. *International Journal of Research and Reviews in Applied Sciences*, 8(2), 194–206.
43. ASTM D790-17. (2017). *Standard Test Methods for Flexural Properties*. ASTM International.
44. Bickerton, S., & Advani, S. G. (1999). Modeling of liquid composite molding processes. *Composites Science and Technology*, 59(14), 2215–2229.
45. Starr, T. F. (2000). *Pultrusion for Engineers*. Woodhead Publishing.
46. ASTM D256-10. (2010). *Impact Resistance of Plastics*. ASTM International.
47. ASTM D2240-15. (2015). *Durometer Hardness Test*. ASTM International.
48. ASTM D570-98. (2010). *Water Absorption of Plastics*. ASTM International.
49. ASTM D618-13. (2013). *Conditioning Plastics for Testing*. ASTM International.

50. ASTM C618-19. (2019). *Fly Ash Specification*. ASTM International.
51. ASTM C1240-14. (2014). *Silica Fume Specification*. ASTM International.
52. Friedrich, K., & Almajid, A. A. (2013). Manufacturing aspects of advanced composites. *Applied Composite Materials*, 20(2), 107–128.
53. ASTM D2344-16. (2016). *Short-Beam Strength of Composites*. ASTM International.
54. Kim, J. K., & Mai, Y. W. (1998). *Engineered Interfaces in Fiber Reinforced Composites*. Elsevier.
55. Srivastava, V. K. (1988). Effect of silane coupling agents on fly ash composites. *Journal of Materials Science*, 23(10), 3690–3696.

About the Book

Engineering Epoxy-Based Glass Fiber Reinforced Hybrid Composites with Industrial Waste Fillers: Materials, Fabrication and Mechanical Performance presents a focused study on developing high-performance, sustainable composite materials by integrating E-glass fiber reinforced epoxy with industrial waste fillers such as fly ash and silica fume. The book systematically covers material selection, hand lay-up fabrication, curing processes, and detailed mechanical characterization based on ASTM standards. It highlights the influence of filler content on tensile, flexural, impact, and hardness properties, and identifies optimal performance at 5 wt% filler loading. The inclusion of TOPSIS-based multi-criteria decision analysis further strengthens the selection of the best composite. Emphasizing both performance enhancement and environmental sustainability, the book is highly relevant for structural applications such as rail joints and serves as a valuable reference for researchers, academicians, and industry professionals.

Key Features:

This book integrates sustainable waste materials into advanced composite design, offering a clear experimental methodology using hand lay-up techniques and standardized testing. It provides comprehensive mechanical performance analysis, identifies optimal filler content, and explains microstructural behavior and interfacial bonding. The application of TOPSIS for material selection adds practical decision-making value. With a strong focus on real-world applications and eco-friendly engineering, the book is well-suited for academic research, industrial use, and advanced studies in composite materials.

Scan this QR Code &visit us:

Published by:
The Institute for Innovations in Engineering and Technology (IIET)
www.theiiet.com
contact@theiiet.com

ISBN 978-8-19-934040-4